TECHNIQUES FOR AUTOMATING LITHOFACIES MAP CONSTRUCTION FOR PRESENTING PALEOGEOGRAPHIC RELATIONSHIPS WITHIN THE EARTH'S SUBSURFACE

by
Christopher D. Bader
B.S., Fort Hays State University, 1985

Submitted to the Department of Geography and the Faculty of the Graduate School of the University of Kansas in partial fulfillment of the requirements for the degree of Master of Arts.

Professor in Charge or Chairperson

Committee Members

Date thesis accepted

Kansas Geological Survey
Open-file Report

Disclaimer

The Kansas Geological Survey does not guarantee this document to be free from errors or inaccuracies and disclaims any responsibility or liability for interpretations based on data used in the production of this document or decisions based thereon. This report is intended to make results of research available at the earliest possible date, but is not intended to constitute final or formal publication.

ABSTRACT

Two-dimensional lithofacies map series are used to present paleogeographic relationships within the earth's subsurface. The volume of data and the complexity of extracting three-dimensional and temporal relationships from stratigraphic data generally prohibits manual construction of lithofacies map series. A lithofacies map series was constructed for the Lansing-Kansas City (LKC) L zone cycle surrounding the Triangle field area using techniques developed as a part of this research. The stratigraphic data were correlated to a time base, and individual map images representing horizontal slices through the vertical stratigraphic sequence were generated using a combination of interpolation operators. The resulting images were compared to manually constructed images to determine the effectiveness of the automated procedures. Since the manual construction processes were based upon subjective interpretation, there was no basis for a quantitative comparison. Therefore, additional factors derived from the underlying conceptual model were also used to evaluate the paleogeographic images, such as system continuity, temporal evolution, and regional trend.

The results of the comparison identified the strengths of the automated reconstruction techniques. The automated techniques use simple mathematical relationships to identify the paleogeographic distribution of the facies. As a result, the automated techniques provide an effective capability for processing three-dimensional stratigraphic data and presenting it within the context of the temporal depositional cycle. The two-dimensional map series generated using these techniques provided a reasonable estimation of the stratigraphic distribution within the context of the depositional cycle. One problem with the automated technique was that it did not

provide any utility for incorporating phenomena that are not specifically identifiable from the data itself, such as the regional geological trend. Ultimately, the automated techniques can augment manual techniques providing effective and reliable processing of complex three-dimensional data sets.

ACKNOWLEDGEMENT

The author would like to express appreciation to the following individuals for their guidance, suggestions, and support. Special thanks to my advisor and chair of my committee Dr. Ling Bian for the assistance and patience through the planning, development, and completion of this work. Thanks to the members of my committee: Dr. Terry Slocum, Dr. Robert Buddemeier, and Dr. Lynn Watney for guidance and support through the review process. I would also like to thank Royce Cline of the North Dakota State Water Commission for his suggestions on the interpolation methodologies that were implemented in this study.

I would also like to express my appreciation to the North Dakota State Water Commission and Milt Lindvig, Director of Water Appropriations of the North Dakota State Water Commission, for the use of the computer hardware and software that was instrumental in the completion of this work.

Finally, this thesis is dedicated to my daughter, Samantha, who gave up much of my time during the completion of this work.

TABLE OF CONTENTS

TABLE OF CONTENTS (Cont)

LIST OF FIGURES

LIST OF FIGURES (Cont)

Page

Figure

LIST OF FIGURES (Cont)

Page

Figure

LIST OF FIGURES (Cont)

Page

Figure

LIST OF TABLES

Chapter One

INTRODUCTION

Western Kansas is a prolific oil producing region with numerous productive stratigraphic zones. The Lansing-Kansas City (LKC) Groups, which are of upper Pennsylvanian age, are some of the more prominent producing stratigraphic zones within the region (Figure 1.1). The productive features of the LKC Groups are commonly small and are predominantly the result of depositional processes. Since the nature of the depositional features makes exploration for productive features difficult when using conventional two-dimensional mapping methods, the key to successfully exploring these types of features lies in the reconstruction of the physical geography of the marine environments and the evolution of these environments throughout the deposition of the LKC Groups (Bader, 1989).

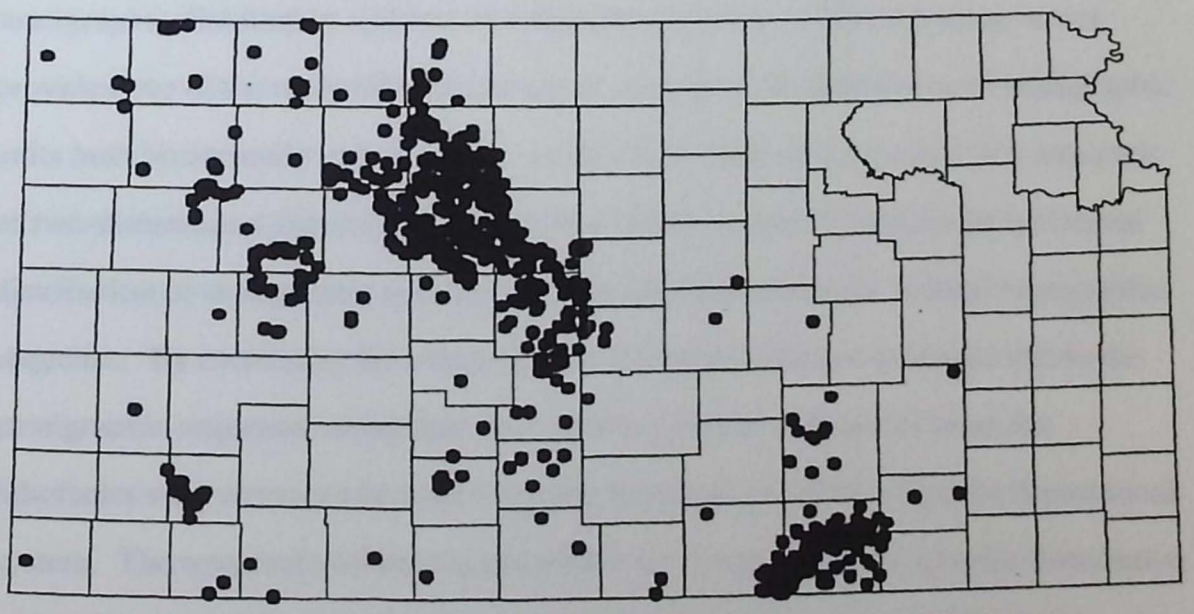

Figure 1.1 - Map of leases with oil and gas production from the upper Pennsylvanian LKC Groups in Kansas (Beene, 1993).

Paleogeographic maps are used in geological investigations for purposes of identifying historic geographic environments. A paleogeographic map is formally defined by Bates, et. al. (1984) as "a map that shows the reconstructed physical geography at a particular time in the geologic past". Paleogeographic maps can be used to portray a wide variety of information, such as the distribution of land and seas, depth of the sea, and climatic conditions. One of the more common tools used to portray paleogeographic conditions is the lithofacies map. Lithofacies maps are used to identify the spatial distribution of different lithologic or stratigraphic units within a defined subsurface horizon. By demonstrating the aerial distribution of different lithologic units, the lithofacies map provides the means for presenting the geographic regions where similar depositional conditions prevailed, which in the case of the LKC Groups is essentially a geographic map of the marine environments.

While a lithofacies map provides an effective tool for presenting the stratigraphic distribution within a two-dimensional plane, a lithofacies map series provides one of the more effective means of presenting the distribution of stratigraphic units both horizontally and vertically. A lithofacies map series consists of a sequence of two-dimensional lithofacies maps; each of which is used to identify the horizontal distribution of stratigraphic units for a selected horizon within the vertical stratigraphic sequence. By correlating the stratigraphy to a temporal datum established within the stratigraphic sequence, rather than to an arbitrary datum such as elevation, the lithofacies map series can be used to portray temporal evolution within the depositional system. The temporal evolution is interpreted by changes in the geographic distribution of the lithologic units which infers change in the geography of the environments responsible for deposition of the different lithologic units.

Construction of a two-dimensional lithofacies map series is not extremely difficult to conceptualize; however, manual construction is generally unfeasible because of the volume of data and the complexities associated with visualizing three dimensional systems. Automated systems, such as geographic information systems (GIS), may provide an acceptable solution for dealing with the volume of data required for map construction. However, most existing or "conventional GIS" do not provide capabilities for analysis or display beyond the dimensions of the x-y plane. Introduction of all three spatial dimensions (x, y, z) and the temporal dimension (t), which is a requirement for reconstructing the paleogeography of the LKC system, severely restricts the utilization of GIS to effectively analyze and model the subsurface system.

Purpose and Objectives

The purpose of this study is to develop effective modeling techniques for automated construction of a lithofacies map series. While the construction techniques presented in this study could be adapted for a broad range of subsurface studies, construction criteria are uniquely fit to lithofacies map construction. Therefore, this study focuses on the specialized application of two-dimensional map construction unique to stratigraphic analysis of the depositional cycles of the LKC Groups in western Kansas.

The reconstruction techniques discussed in this study will not address the complex issues related to geophysical log analysis techniques. Even though appropriate geophysical analysis techniques are critical for any accurate or detailed

reconstruction, discussion of these issues would extend beyond the scope of this study. The discussion presented in this study focuses on the design of the automated reconstruction techniques and associated problems. The data used for reconstruction purposes is assumed to have been defined by a trained geologist with expertise and working knowledge of geophysical analysis techniques and an understanding of depositional stratigraphy as it pertains to the LKC system.

In order to develop an effective construction capability that provides a means of automating analysis and display for the spatial (x, y, z) and temporal (t) dimensions within the stratigraphic system, the following tasks were considered.

1) A data structure capable of preserving the accuracy and reliability of the well data while providing adequate representation of the lithofacies map series for a range of scales.

2) Temporal analysis techniques capable of identifying temporal events within the stratigraphic system (i.e. depositional events, sedimentation cycles, stratigraphic correlation, etc.).

3) Three-dimensional interpolation capable of identifying the stratigraphic distribution within the framework of both the horizontal and vertical dimensions.

4) An effective mechanism for presenting the model output for appropriate display of the complex stratigraphic relationships in the form of a lithofacies map series.

Chapter Two

LITERATURE REVIEW

The literature reviewed for this study can be divided into two broad categories: (1) background of the methods and techniques that are appropriate for automating the lithofacies map construction, and (2) the background related to the underlying geological concepts for which the automated techniques are applied. While this study clearly focuses on the techniques for automating the construction of the lithofacies maps, the underlying geological model used as the basis for the manual construction techniques must be presented to provide an appropriate context within which to develop the automated techniques.

Modeling Techniques

Geo-scientists have long been faced with the problems and complexities associated with analysis and display of three-dimensional systems. A variety of tools have been implemented in efforts to conceptualize, model, and display three-dimensional relationships associated with subsurface systems. As technology has evolved, more and more capable computer hardware and software have been developed to aid geo-scientists in modeling subsurface systems. Van Driel (1989) divided computer techniques for study in geology into three broad classes based upon their complexity: two dimensional analysis and display, three dimensional display, and three dimensional analysis. While two dimensional analysis and display

techniques have been used by geo-scientists for years, three-dimensional display and three dimensional analysis techniques are not yet readily available.

Two-dimensional techniques have evolved from software for computer graphics, image processing, and more recently from GIS (Van Driel, 1989). While GIS provides an effective means of modeling spatial systems, the technology has not evolved sufficiently to address the display and analysis capabilities required to effectively model complex three-dimensional geological problems. True three-dimensional display would provide the user with visualization tools that would lead to a better understanding of complex phenomena (Smith, et. al., 1989). In current GIS technology, three-dimensional display capabilities are generally limited to perspective or "2.5-dimensional" views where attribute relationships are draped over a two-dimensional surface (Davis, et. al., 1989). While a perspective view provides useful information, a perspective view does not adequately convey true three-dimensional relationships. In many cases, current GIS technology fails to adequately model three-dimensional or solid bodies because of the underlying problems associated with adapting two-dimensional tools to three-dimensional problems. Ris (1991) identified many of the areas in which traditional two-dimensional methods must be replaced by methods more appropriately designed for scientific applications. Some of the areas Ris (1991) discussed are related to the focus of this study, such as temporal and three dimensional data models, event recognition, spatial and temporal interpolation, and visualization.

Data Models

One of the primary difficulties in modeling the subsurface lies in the development of data models that adequately define the spatial relationships of three-dimensional systems (Jones, 1989). Aronoff (1989) identified the raster model and the vector model as the two fundamental data models used for representation of the spatial component of geographic information. The raster model, as defined by Aronoff (1989), "consists of a regular grid of square or rectangular cells" where the location of each cell is defined by its row and column. The vector model, on the other hand, utilizes coordinate positioning to identify points, lines, and polygons that represent spatial features (Aronoff, 1989).

Most existing or "conventional GIS" handle two-dimensional data with either grid-based or vector-based models, but generally do not provide capabilities for storage or analysis of either the third spatial dimension or the temporal dimension. Langran (1989) reviewed relevant research on temporal database design only to point out that a single definitive blueprint does not exist, and creation of temporal database capabilities will require specialized design to fit individual applications. Jones (1989) identified similar problems with developing a comprehensive model for three-dimensional systems.

Jones (1989) examined voxel structures for purposes of accessing and retrieving three-dimensional data associated with geological systems. A voxel model is essentially a three-dimensional version of a grid or raster model with a volumetric or cube-based structure rather than a flat cell-based structure (Figure 2.1). Voxel models generally provide simpler data structures with easier access than a comparable

topological model; however, the nature of the voxel structure results in very large storage requirements. Various storage schemes can be applied to the voxel structure to reduce storage size and increase overall performance when accessing the structure. An octree, which is similar to the two-dimensional counterpart, the quadtree, is an example of a storage scheme used to reduce the storage demands of the voxel structure (Figure 2.1).

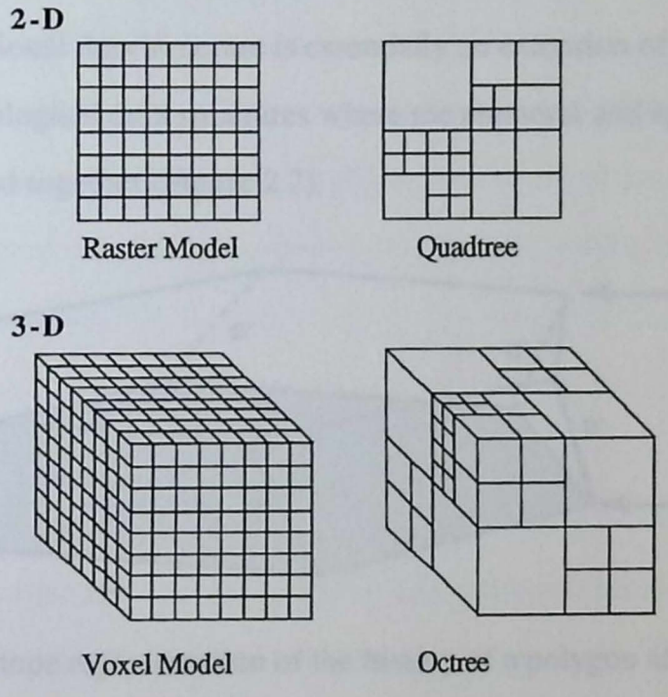

Figure 2.1 - The raster and quadtree models provide an efficient means of segmenting 2-D regions for purposes of spatial indexing. The voxel and octree models are the 3-D equivalents of the raster model and the quadtree (Jones, 1989).

One of the major disadvantages of using a voxel structure lies in the selection of an appropriate voxel resolution to adequately model the data (Jones, 1989). This is similar to the problem of selecting an appropriate grid cell resolution within a two-dimensional system, in that a fine resolution may adequately represent the heterogeneity of the data, but may require such storage overhead as to be unusable.

The reverse situation would be a coarse voxel structure that is efficient to use, but can not be used to identify complexities associated with the system represented by the model.

Hazelton, et. al. (1990) described a four-dimensional topological model that provides a means of storing temporally referenced, three-dimensional information. The four-dimensional data structure is essentially an extension of conventional two-dimensional topological data structures where the temporal and spatial components of the data are stored together (Figure 2.2).

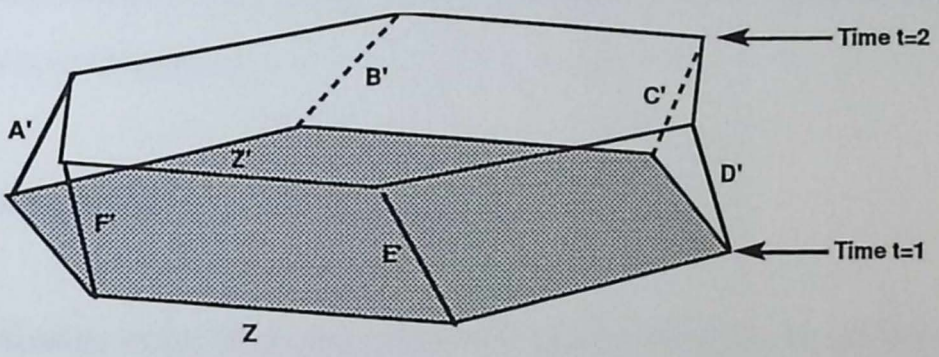

Figure 2.2 - Polytope representation of the history of a polygon after Hazelton, et. al. (1990). The polyhedron represents the changes in the base hexagon at time t=1 to time t=2. Lines A' through F' represent the path of each of the nodes of the hexagon from time t=1 to t=2.

Even though the four-dimensional topological structure is derived from conventional structures, the creation, storage, and management of a higher order topological relationship is far more complex. The higher order topological structure makes the concept of 'left' and 'right' polygons obsolete and requires the recreation of the topological structure as part of the software rather than within the data structure as in "conventional GIS" (Hazelton, et. al. 1990). While this approach may effectively

reduce storage and structure demands upon the data structure, it dramatically increases the complexity of the modeling process.

Youngmann (1989) examined both types of spatial data structures as they are applied to general subsurface modeling and concluded that the topological structure offers the greatest potential for addressing data complexities. However, Youngmann (1989) also indicated that the topological structure introduces greater complexities for development and maintenance of the model while the voxel or raster based structures provide greater ease and flexibility of implementation. In either case, selection of an appropriate structure must be determined by the type of application for which the structure is to be applied.

Event Recognition

Another major issue facing scientific applications is the ability to process data to facilitate recognition of phenomena or events within the data (Ris, 1991). Beller (1991) defined an event as an object that has spatial and temporal extents and has meaning to the user. The basic object for analysis of a temporal event will be the map time slice series or the temporal map set (Beller, et. al., 1991). The temporal map concepts were formally defined by Beller et. al. (1991):

" ***Map Time Slice*** *A map layer for a specific geographic area and theme at a specific time.*

Temporal Map Set (TMS) *A map layer covering a period of time (i.e. a set of time slices covering the same geographic area and theme)* "

Establishing the temporal reference for an event requires the capability to recognize change as a function of time; this predicates the capability to recognize the start, end, and relative points within the event (Beller, 1991). Two different types of temporal logic have been described for analyzing temporal events; a change-based approach, and a time-based approach (Al-Taha, et. al. 1990). The change-based approach does not explicitly address the time domain, and as a result, time is implicitly recorded as changes are observed. The time-based approach considers time as a separate dimension and recognizes only one basic change; "the passage of time". There are numerous limitations to a change-based approach that present major difficulties for developing adequate temporal logic, and in most applications, the time-based approach is considered to be more appropriate (Al-Taha, et. al. 1990). However, subsurface environments, where time is often inferred from the vertical dimension, are ideal for utilization of a change-based logic.

Three-Dimensional or Temporal Interpolation

An important step in the development of a three-dimensional subsurface model is the reconstruction of the spatial distribution of subsurface phenomena. This task is difficult because the control data occur in the form of scattered observation points established by wells and test holes that penetrate the substrate. As a result, elaborate computerized techniques have evolved for interpreting subsurface relationships. While applications of three-dimensional interpolation techniques are not widely discussed in the literature, the problems associated with developing an integrated three-dimensional model of the subsurface is similar to the simpler case of developing a map for representing two-dimensional surfaces from sparse control points.

There are numerous forms of surface and subsurface mapping techniques used by geo-scientists. Of the many types of maps, contour maps are generally the most commonly applied in geology for purposes of defining subsurface relationships (Davis, 1986). A contour map is generally defined to contain isolines of equal value (Davis, 1986), and regardless of the phenomenon intended for display, the primary objective of the contour map is to present some relationship within the surface or subsurface. Historically, contour maps were generated entirely by hand. However, with the introduction of computers, an alternative to the laborious manual techniques was introduced, and the computer has become a valuable mapping tool (Jones, 1986).

In order to develop a contour map on a computer, a mathematical model must first be constructed that provides a means of estimating the surface form from scattered control points. Over the past two decades, a wide variety of mathematical interpolation models have evolved to provide more efficient and effective tools for developing various forms of maps (Davis, 1986; Burrough, 1986; Jones, 1986). Burrough (1986) classified interpolation models into two broad categorical types: discrete, and non-discrete. Models based upon discrete functions generally assume that all important variation occurs at boundaries; within the boundaries, no variation occurs. Discrete interpolation models include such things as Thiessen polygons. Models based upon non-discrete functions assume continuous spatial change that can be described by a smooth mathematically defined surface. These types of models include spline functions, trend-surfaces, Fourier series, moving averages, and kriging. Both types of interpolation techniques have been extensively applied within the geo-sciences; Davis (1986) and Burrough (1986) provide detailed explanations of most of these techniques as they are applied to geographic problems.

While interpolation models and computerized map production have evolved, there is still considerable debate as to the functionality of the interpretation produced by computerized techniques. Computerized mathematical-based models lack the ability to incorporate intuitive knowledge, but computerized methods reduce the biases introduced through manual methods. Davis (1986) discussed the merits of geological interpretation and indicated that in some instances the addition of geologic interpretation to the raw data contained in the observation points can significantly enhance the map while in other instances personal bias can detract rather than add to the utility of the map.

Dahlberg (1972, 1975) investigated the utility of computer mapping by preparing a test case where duplicate datasets of a known area were given to experienced geologists. The maps produced by the geologists were then compared to the results of a computer generated map and the known map. Dahlberg concluded that while the geologists interpretations varied, the computer provided an effective average of the various interpretations developed manually. Davis (1986) and Jones (1986) both stated that while computer developed maps may not incorporate geological bias into their interpretation they still represent an improvement over manually generated maps because, in addition to the efficiency that the computer provides, the maps developed using computerized techniques are reproducible, consistent, and objective. While computerized maps may not provide interpretative capabilities that equal that of trained and experienced scientists, computer mapping does provide a means of developing complex data sets to produce an initial interpretation which can then be refined by trained geologists.

In recent years, considerable effort has been devoted to developing more realistic mathematical models of surfaces (Green, et. al., 1978; Yoeli, 1978; Elfick, 1979; McCullugh, et. al., 1980; Burrough, 1986, and others). However, Jones (1986) suggests that, while better mathematical models have provided better interpretive tools, a more concerted effort should be made to integrate existing interpolation models with manual interpretative processes. Jones (1986) maintained that this approach may actually yield better results with less effort than improving existing mathematical models.

Visualization

Visualization is a key component of most scientific applications in which it provides the only mechanism for reviewing complex data relationships by manipulating and exploring data in a manner not otherwise possible. DiBiase (1991) best described the goal of visualization in scientific computing which is to "leverage existing scientific methods by providing new scientific insight through visual methods". Visualization of scientific data has been the focus of much research in recent years primarily resulting from needs within the scientific community coupled with cheaper more powerful computer capabilities. Visualization of complex surface relationships is finally extending beyond the simple "2.5 D" or perspective view (Davis, et. al., 1989) to include more sophisticated and more demanding forms of display: animation (Moellering, 1980), 3-dimensional projections on 2 or 2.5 dimensional surfaces (Junkin, 1982), and in the future, interactive volumetric display that is already beginning to appear in software packages like Spyglass Dicer, developed by Spyglass, Inc.

Conventional static maps provide a viewpoint at a specific point in time (Moellering, 1980), and the temporal map set provides a means of displaying temporal evolution where each map resembles a frame in a movie. The temporal map set can be displayed as an animated sequence or as a static map series where individual map images are all displayed simultaneously. Within a temporal map set, the design of the individual images remains constant so that attention is devoted to the shifts in the data rather than the presentation format. This approach is similar to the concept described by Tufte (1983) as small multiples where change is demonstrated by a group of similarly constructed images that are indexed by change in another variable. While individual frames define a changing phenomena, the constancy of design of the images places the emphasis on changes in the data (Tufte, 1990).

Geological Background

The LKC Groups were deposited in a low to moderate energy, shallow (epeiric) sea that extended over much of western Kansas, eastern Colorado, and northwestern Oklahoma during the upper Pennsylvanian period (Figure 2.3) (Watney, 1980). The broad epeiric basin sloped gently toward the Anadarko Basin to the south. Oil and natural gas production from the LKC Groups in the western Kansas region is derived from two different types of facies that were prominent deposits in the epeiric seas: the algal mound facies, and the oolitic shoal facies. The algal mound facies consists primarily of the accumulation of skeletal carbonate remains of various types of benthic fauna including phylloid algae. The oolitic shoal facies consists of carbonate oolitic grains that were generated and distributed as wave energy and current action were imposed on the sea-floor.

Periodic sea-level changes throughout the accumulation of the LKC Groups produced a cyclical stratigraphic sequence. Irwin (1965) and Watney (1980) identified mechanisms of the regional depositional system that controlled deposition of the LKC Groups and the development and distribution of the algal mound and the oolitic shoal facies. These mechanisms provided the basis for the predictive depositional model developed by Bader (1989) to define potential algal mound and shoal facies development within the northern portion of the shelf.

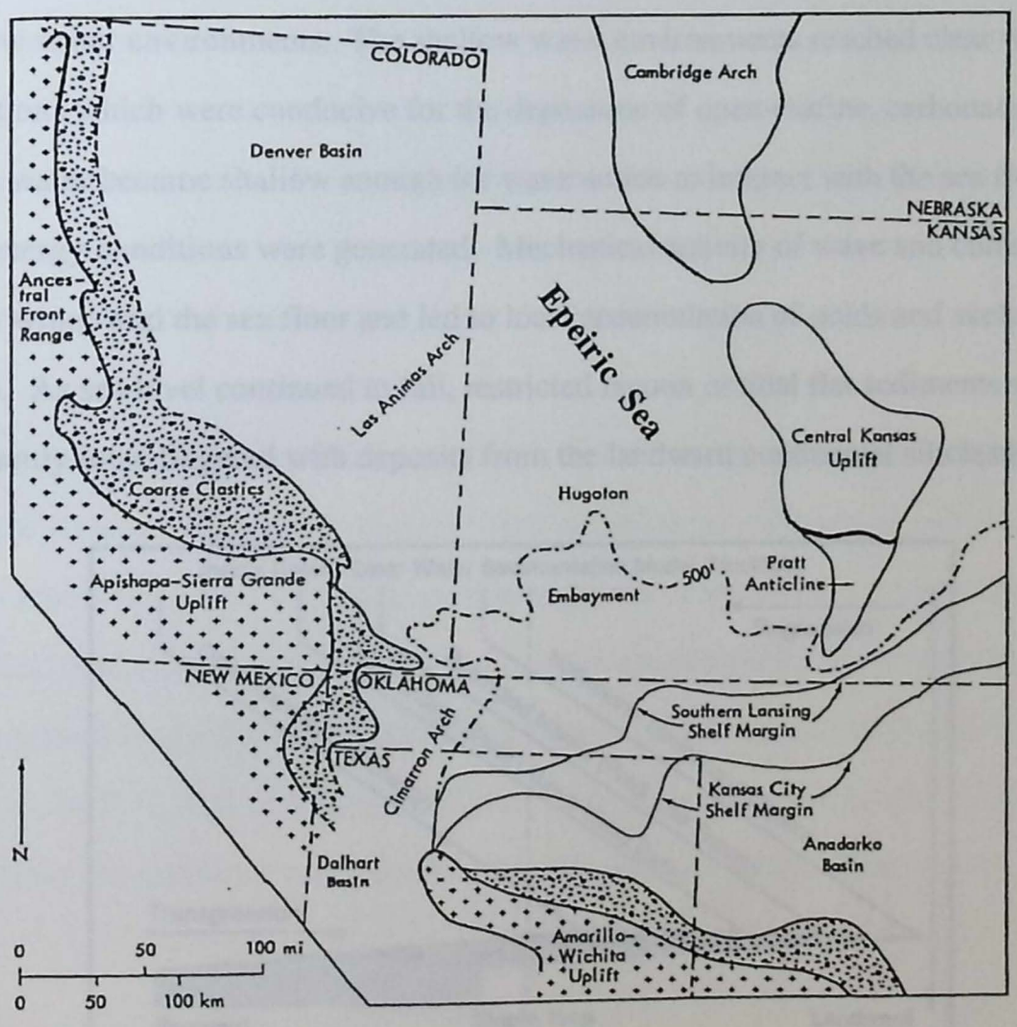

Figure 2.3 - Missourian paleogeographic map of western Kansas and adjacent areas (adapted from Watney, 1980).

Regional Depositional System

The depositional environment within the epeiric seas of the western Kansas platform exhibited a high degree of variability (Figure 2.4). Facies shifted landward and basinward in response to the periodic changes in sea level. Low-energy zones, in which marine shales were deposited, existed during times of greatest inundation (Watney, 1980). As water shallowed, facies shifted basinward which created a transitional regime between the lower energy deeper marine environment and the shallow water environments. The shallow water environments reached clear water conditions which were conducive for the deposition of open-marine, carbonates. When water became shallow enough for wave action to interact with the sea floor, high energy conditions were generated. Mechanical activity of wave and current action winnowed the sea floor and led to local accumulation of ooids and skeletal grains. As sea level continued to fall, restricted lagoon or tidal flat sediments were commonly inter-fingered with deposits from the landward continental siliclastics.

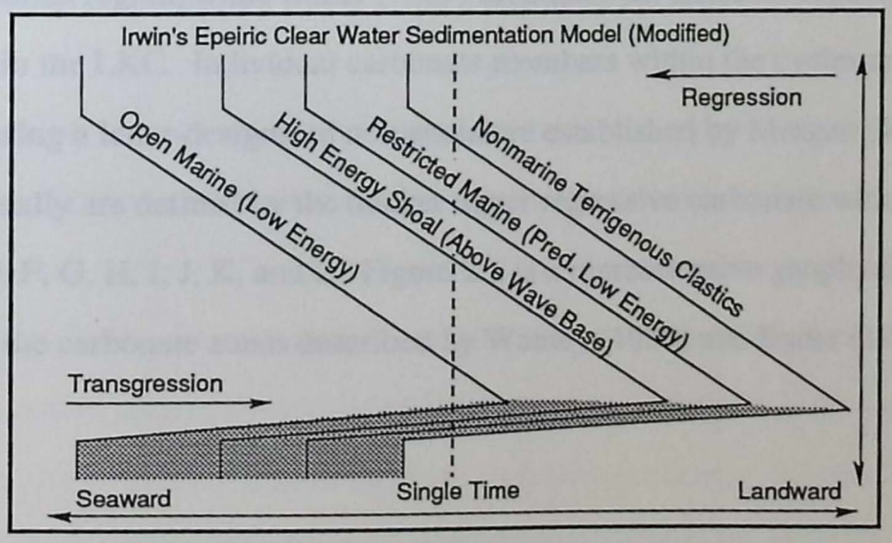

Figure 2.4 - Modified version of Irwin's epeiric, clear-water sedimentation model (adapted from Watney 1980).

Regional sea-level fluctuations forced the environmental regimes to migrate landward and seaward (Irwin, 1965). The migration of the depositional environment landward and seaward created the cyclical transgressive-regressive depositional system that was responsible for the repetitive stratigraphic sequence of the LKC Groups. The transgressive phase of the depositional cycle, characterized by the landward advance of the sea and the associated landward migration of the depositional environments, initiated each of the depositional cycles. The regressive phase of the depositional cycle, characterized by the retreat of the seas and the associated seaward migration of the depositional environment, completed each of the depositional cycles. Each of the depositional cycles in the LKC interval in western Kansas is represented by four basic stratigraphic members in ascending order: a thin transgressive carbonate, a thin marine shale, a dominant, thicker regressive carbonate, and finally a regressive shale that is variable in thickness (Figure 2.5).

Watney (1980) identified as many as nine different depositional cycles in the northern Kansas region, while Bader (1989) identified ten different depositional cycles within the LKC. Individual carbonate members within the cycles are generally described using a letter-designated nomenclature established by Morgan (1952). The cycles generally are defined by the thicker upper regressive carbonate which includes the A, C, D, F, G, H, I, J, K, and L. Figure 2.6 is a representative geophysical log identifying the carbonate zones described by Watney (1980) and Bader (1989).

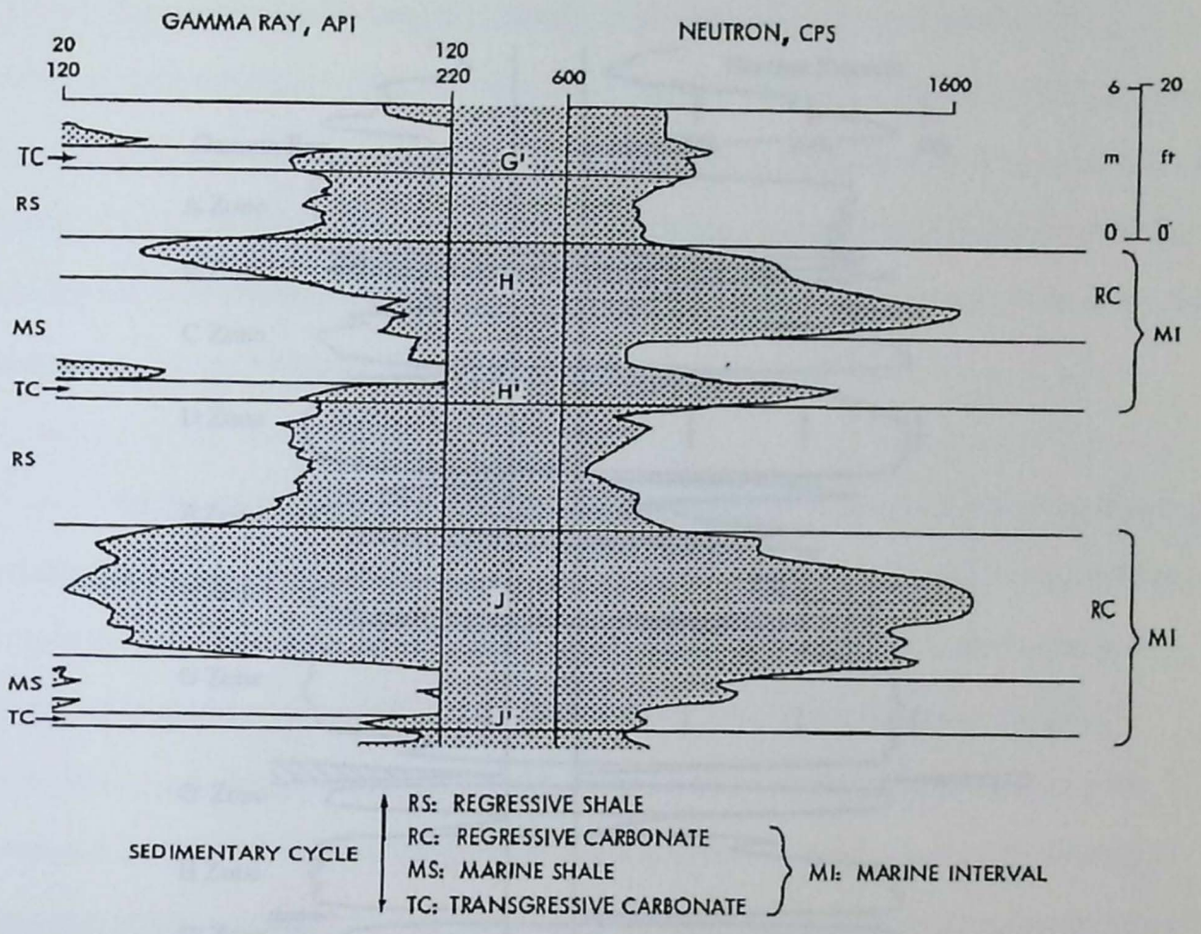

Figure 2.5 - Representative geophysical log depicting the stratigraphic members of the LKC transgressive-regressive stratigraphic cycles (adapted from Watney, 1980).

The transgressive phase of each depositional cycle, consisting of the thin transgressive carbonate member (Figure 2.3), is attributed to a rapid landward shift of the shoreline and submergence of the shelf in response to a relatively rapid rise in sea-level (Watney, 1980). Watney (1980) indicated that the base of the transgressive carbonate member closely approximates a time surface. The base of the transgressive carbonate is also a shelf-wide subaerial exposure surface creating "temporal distinction" for the depositional cycles. Therefore, in local areas of the shelf, the base of the transgressive carbonate member can be considered as a "zero time" datum for each depositional cycle.

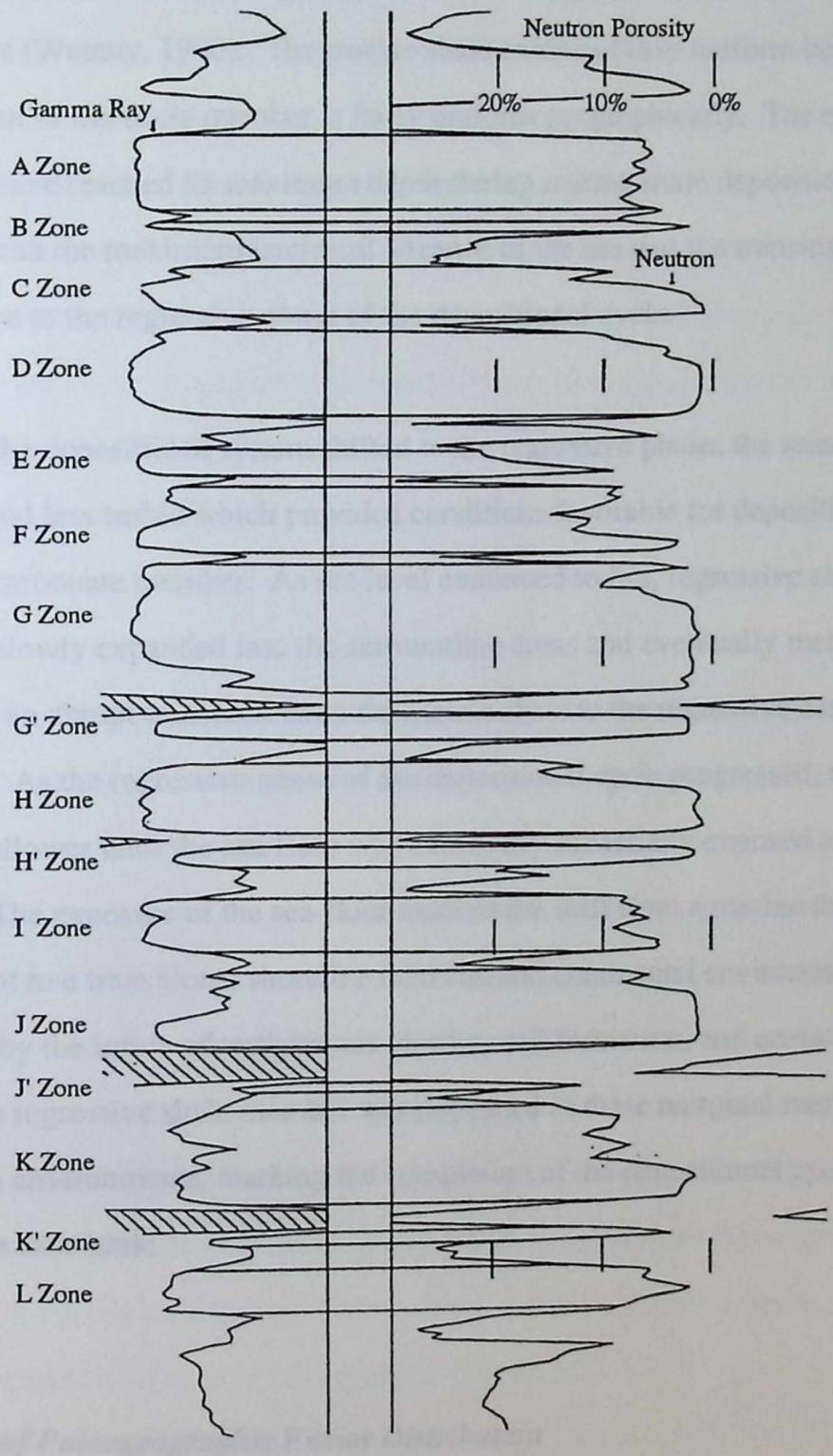

Figure 2.6 - Geophysical log of the #61-25 William Bixenman, showing the letter-designated correlation of the LKC carbonate zones (modified from Bader, 1989).

The marine shale was deposited in a low-energy, subtidal, marine environment (Watney, 1980). The marine shale exhibits fairly uniform bedding, and accumulation of the shale member is fairly uniform geographically. The epeiric sea is inferred to have reached its maximum depth during marine shale deposition, which coincided with the maximum landward advance of the sea and the transition from the transgressive to the regressive phase of the depositional cycle.

As the depositional system shifted to the regressive phase, the seas became shallower and less turbid which provided conditions favorable for deposition of the regressive carbonate member. As sea level continued to fall, regressive carbonate deposition slowly expanded into the surrounding areas and eventually merged, completing an abrupt transition from the marine shale to the regressive carbonate deposition. As the regressive phase of the depositional cycle progressed, the seas became shallower until the sea-floor was eventually subaerially exposed as the seas retreated. The exposure of the sea-floor marked the shift from a marine depositional environment to a transitional shoreline tidal flat and continental environment that was dominated by the influx of terrigineous clastics, soil formation, and erosion (Watney, 1989). The regressive shale member was deposited in these marginal marine and non-marine environments, marking the completion of the depositional cycle and a break in the time scale.

Definition of Paleogeographic Facies Distribution

Productive reservoirs within the LKC Groups reside primarily in the algal mound and oolitic shoal facies. The algal mound and the shoal facies are carbonate

facies that were developed within the regressive carbonate member. Development of the algal mound facies occurred predominantly in the lower and mid portions of the regressive carbonate, while the shoal facies development occurred predominantly within the upper portion of the regressive carbonate. Bader (1989) indicated that the development of both the algal mound and shoal facies was controlled by the configuration of the sea-floor, the relative depth of the sea, and the relationship between the sea-floor and wave and current activity. Since these factors ultimately control the potential for oil recovery from the LKC Groups within the western Kansas region, reconstruction of the paleogeographic environments and the evolution of these environments through time aids in isolating productive trends (Bader, 1989).

Todd (1976) presented a method for reconstructing the history of oolite-bar progradation within the Permian San Andres Formation in the Midland Basin based upon a lithofacies mapping series. Asquith (1979) applied similar techniques for reconstructing the history of oolitic grainstone shoal facies for the Council Grove B-zone in his discussion of depositional models for reconstructing subsurface carbonate environments. Asquith utilized the lithofacies map series to identify the paleogeographic distribution of a shoal facies at specific "slice intervals" above a "bentonite marker" for purposes of demonstrating the depositional evolution of the shoal feature. In the case of both Todd and Asquith, the vertical dimension was used to interpret the historic or temporal evolution of the depositional system in the form of a two-dimensional lithofacies map series (Figure 2.7).

In order to reconstruct temporal changes in lithofacies distribution, i.e. paleogeography, the stratigraphic data must be correlated to a datum that represents an effective time base (Figure 2.7). Asquith (1979) used the "bentonite marker" to

reconstruct the temporal evolution of shoal development. Watney (1980) identified the thin transgressive carbonate member of the LKC system as an approximate time surface. Bader (1989) used the base of the transgressive carbonate as the datum for constructing time slices through the LKC cycles.

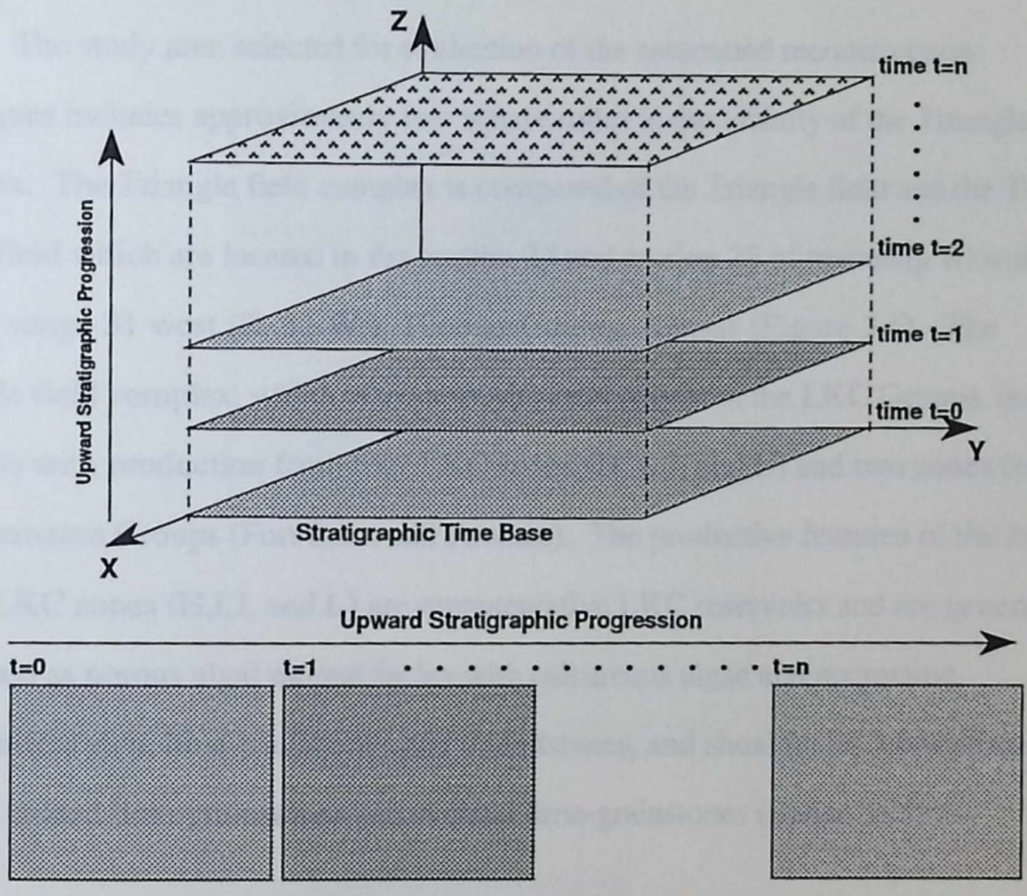

Figure 2.7 - Conversion of vertical stratigraphic sequence to a temporal sequence for presenting the historic aspects of depositional development.

Chapter Three

METHODOLOGY

Study Area

The study area selected for evaluation of the automated reconstruction techniques includes approximately two square miles in the vicinity of the Triangle field complex. The Triangle field complex is composed of the Triangle field and the Triangle North field which are located in the section 24 and section 25 of township 10 south (T. 10 S.), range 31 west (R. 31 W.), Thomas County, Kansas (Figure 3.1). The Triangle field complex, which is a composite reservoir from the LKC Groups, includes 20 wells with production from four LKC zones (H, I, J, and L) and two zones from the Marmaton Groups (Fort Scott and Pawnee). The productive features of the four lower LKC zones (H,I,J, and L) are representative LKC reservoirs and are generally described as porous algal mound facies with calcareous algae and encrusting foraminifera rich, lime-packstones and boundstones, and shoal facies, consisting of Osagia coated lime-grainstones and skeletal lime-grainstones (Bader, 1989).

The Triangle field is typical of western Kansas reservoirs with production from the LKC Groups, in that the field consists of several discrete reservoirs that occur in different horizons within the LKC strata. Most of the wells in the Triangle field produce from fewer than the four LKC zones because of the discontinuous nature of the porosity development. Figure 3.1 identifies the distribution of each of the productive reservoirs in the LKC (H,I,J, and L).

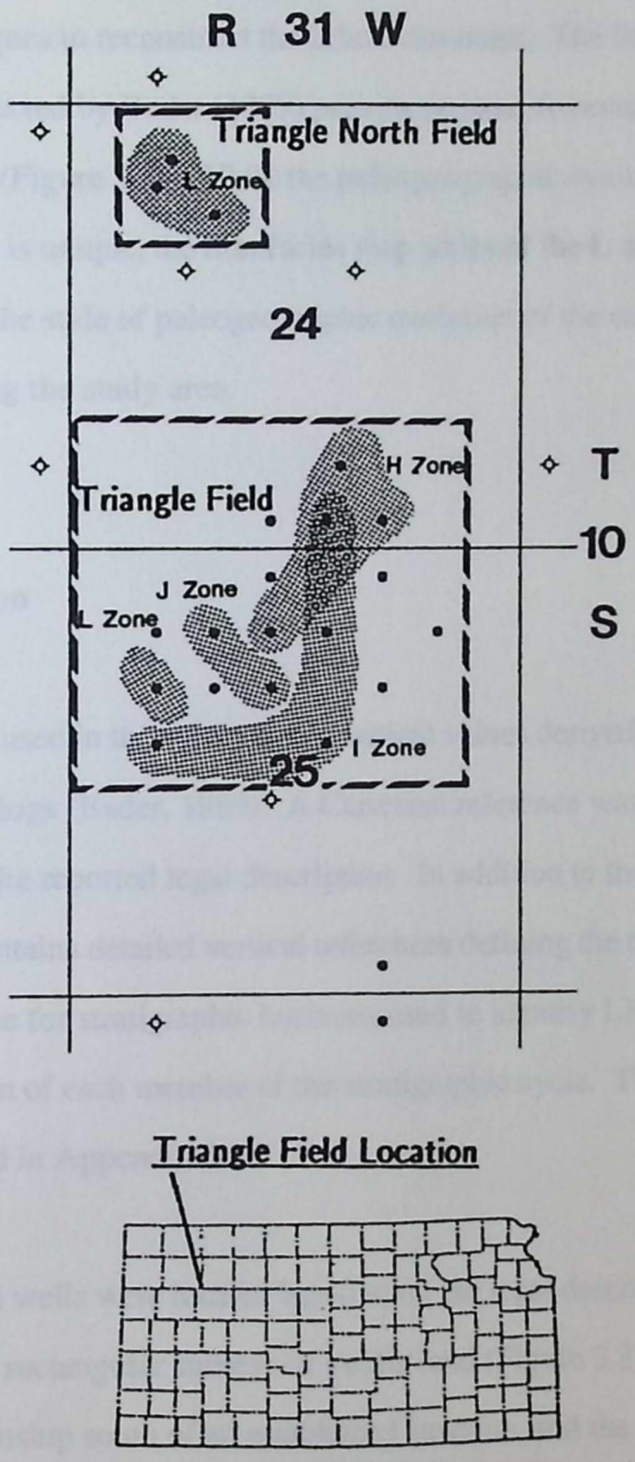

Figure 3.1 - Location of the Triangle field identifying the productive reservoirs from the LKC Groups H, I, J, and L zones.

The L zone cycle in the Triangle field was selected for evaluation of the automated techniques to reconstruct the lithofacies maps. The lithofacies map series previously constructed by Bader (1989) provides a basis for evaluating the automated map construction (Figure 3.2). While the paleogeographic evolution of the Triangle field L zone cycle is unique, the lithofacies map series of the L zone cycle is representative of the style of paleogeographic evolution of the other zones within the region surrounding the study area.

Data Preparation

Well data used in this study are numerical values derived from available geophysical well logs (Bader, 1989). A Cartesian reference was established for each well based upon the reported legal description. In addition to the well location, each data point also contains detailed vertical references defining the elevation and depth below land surface for stratigraphic horizons used to identify LKC features, including the top and bottom of each member of the stratigraphic cycle. The well data used in this study are included in Appendix A.

Individual wells were located based upon the legal description reported in the federal system of rectangular surveys of public land (Figure 3.3). The first number identifies the township south of an established baseline, and the second number identifies the range west of the Fifth Principal Meridian. The third number identifies the section within the designated township and range in which the well or test hole is located. The letters A, B, C, and D designate, respectively, the northeast, northwest, southwest, and southeast quarter section (160 acre tract), quarter-quarter section (40

acre tract), and the quarter-quarter-quarter (10 acre tract). Therefore, a well identified as 10-31-04ADD would be located in the SE1/4 SE1/4 NE1/4 Section 4, Township 10 South, Range 31 West (Figure 3.3). Selected wells were also reported based upon a surveyed distance from a particular section line. For example, 1050'FEL, 1300'FWL would indicate that the well is located 1050 feet from the east section line and 1300 feet from the west section line.

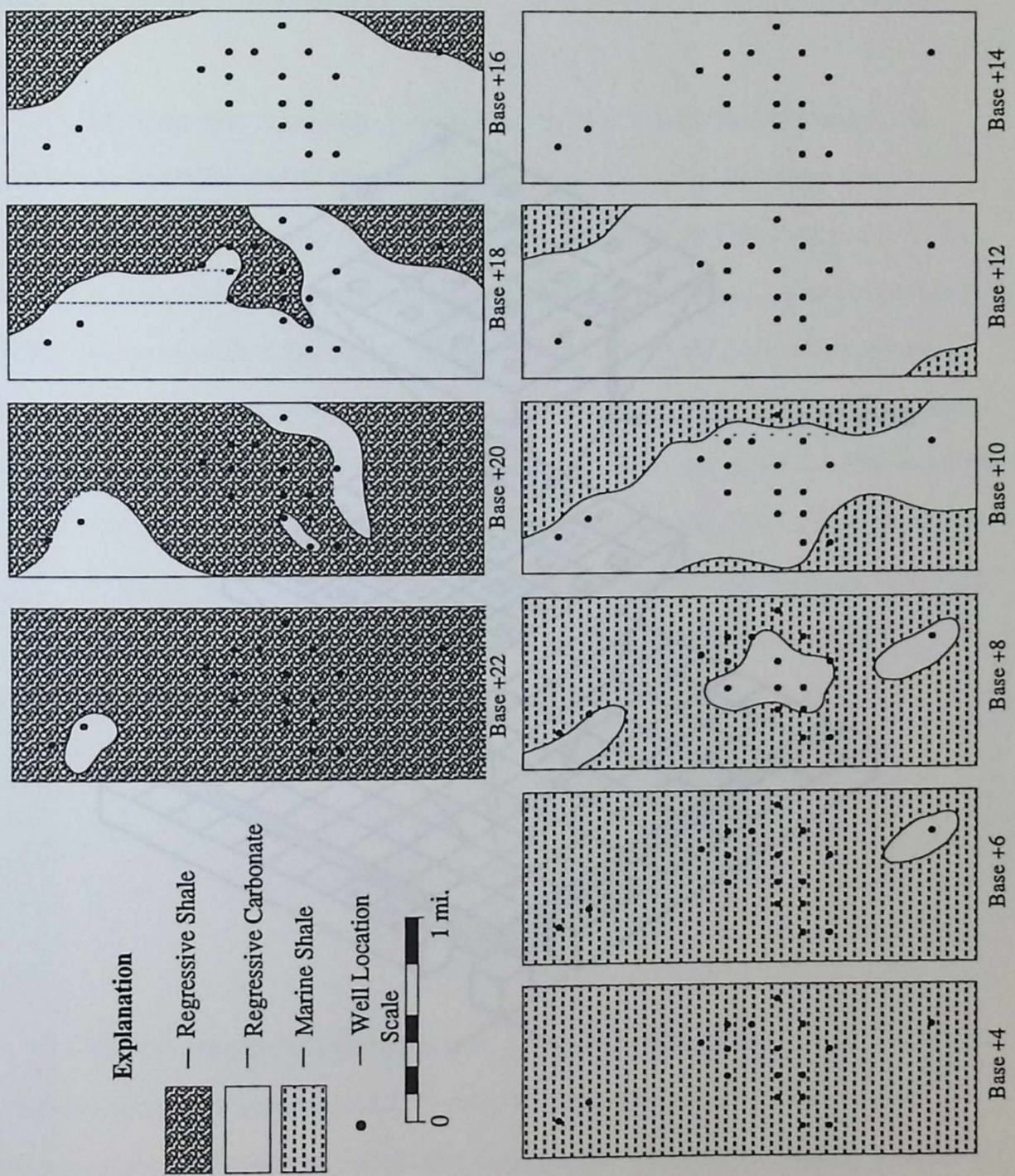

Figure 3.2 - Paleogeographic reconstruction of the Lansing-Kansas City L zone cycle of the Triangle Field using a 2 foot map slice interval. Maps are based upon a stratigraphic sequence that is correlated to the base of the transgressive carbonate member (i.e. Base+4 represents the stratigraphic horizon that is 4 feet above the base of the transgressive carbonate member). Modified from Bader (1989).

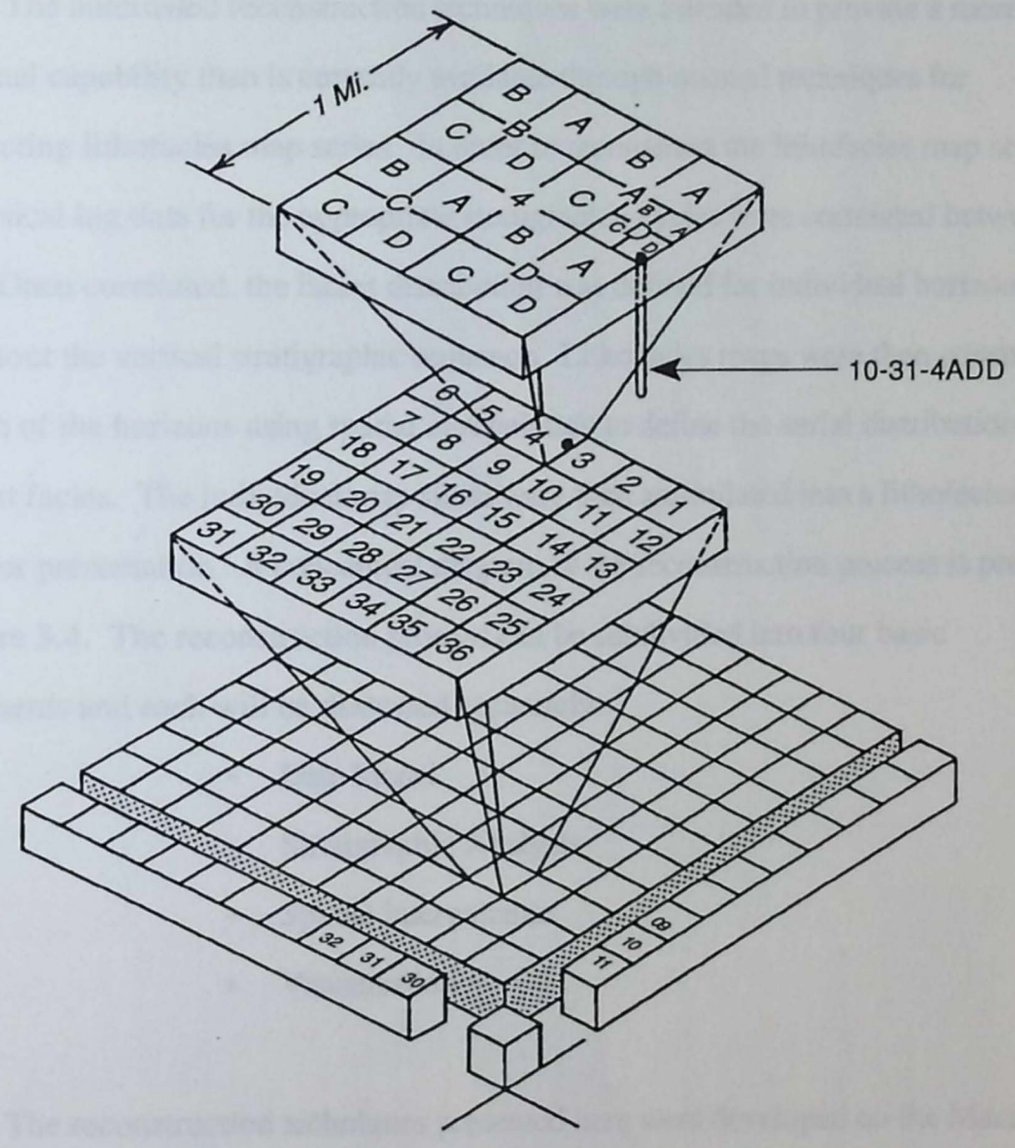

Figure 3.3 - Location descriptions based upon the Federal Land Surveys system.

Reconstruction Techniques

The automated reconstruction techniques were intended to provide a more functional capability than is currently available through manual techniques for constructing lithofacies map series. In order to reconstruct the lithofacies map series, geophysical log data for the appropriate stratigraphic cycles were correlated between the wells. Once correlated, the facies distribution was defined for individual horizons throughout the vertical stratigraphic sequence. Lithofacies maps were then constructed for each of the horizons using spatial interpolation to define the aerial distribution of the different facies. The individual map slices were then assimilated into a lithofacies map series for presentation. A conceptual diagram of the reconstruction process is presented in Figure 3.4. The reconstruction process can be subdivided into four basic components and each will be discussed separately:

- Data Model
- Stratigraphic Analysis
- Spatial Interpolation
- Visualization

The reconstruction techniques presented here were developed on the Macintosh platform because of the availability of fairly low-cost graphics applications. The automated reconstruction of the lithofacies map series was accomplished by integrating various commercial software components, each addressing a portion of the problem. Certain components for which commercial software was not available were developed using 4th Dimension's procedural language and FORTRAN.

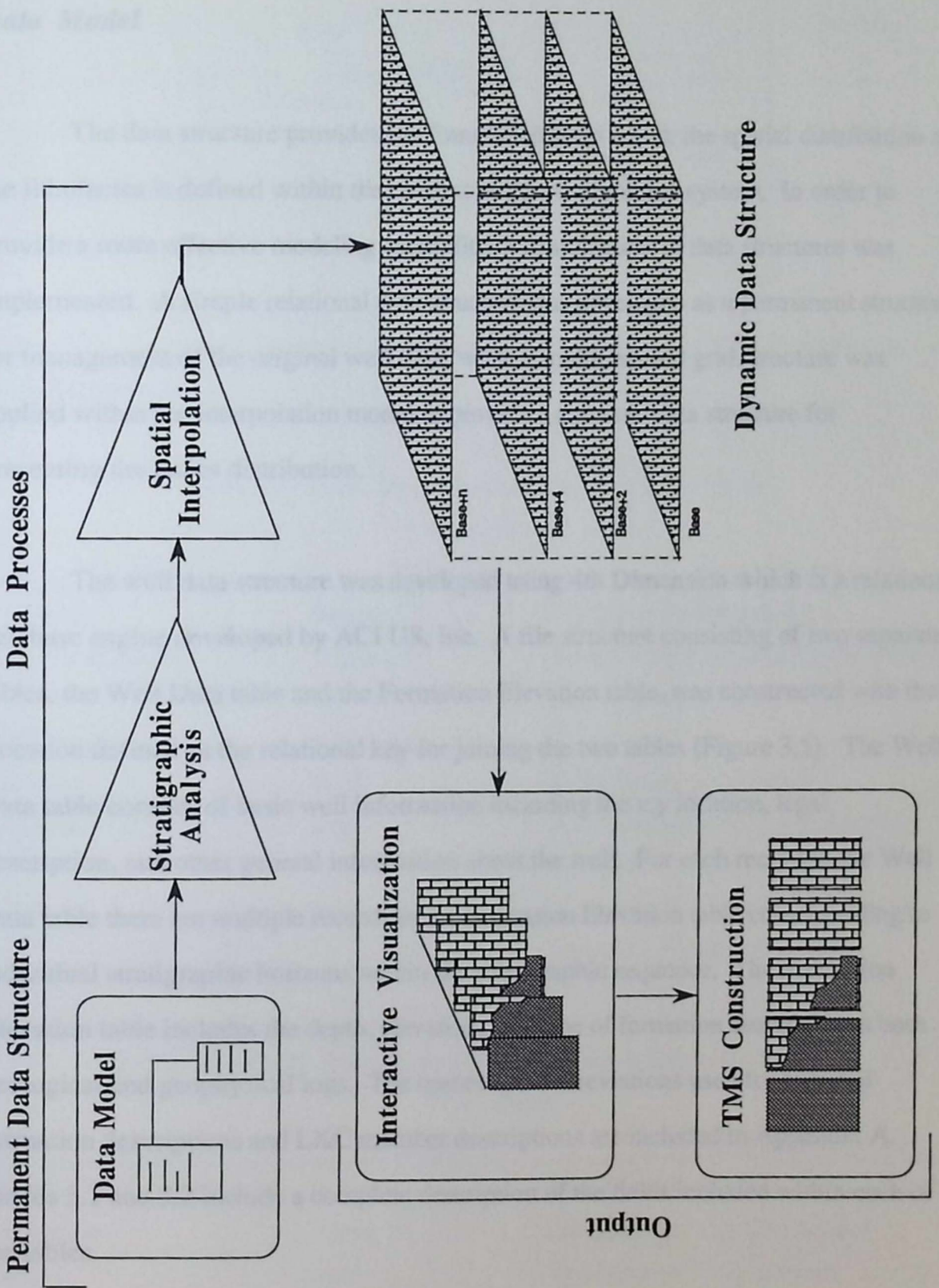

Figure 3.4 - Conceptual diagram of the reconstruction process.

Data Model

The data structure provides the foundation from which the spatial distribution of the lithofacies is defined within the context of the stratigraphic system. In order to provide a more effective modeling capability, a combination of data structures was implemented. A simple relational data structure was developed as a permanent structure for management of the original well data, while a multi-layered grid structure was applied within the interpolation model to provide a dynamic data structure for presenting the facies distribution.

The well data structure was developed using 4th Dimension which is a relational database engine developed by ACI US, Inc. A file structure consisting of two separate tables, the Well Data table and the Formation Elevation table, was constructed with the Location defined as the relational key for joining the two tables (Figure 3.5). The Well Data table consists of basic well information including the x,y location, legal description, and other general information about the well. For each record in the Well Data table there are multiple records in the Formation Elevation table corresponding to individual stratigraphic horizons within the stratigraphic sequence. The Formation Elevation table includes the depth, elevation, and type of formation derived from both geological and geophysical logs. The names and abbreviations used for regional formation descriptions and LKC member descriptions are included in Appendix A. Tables 3.1 and 3.2 include a complete description of the fields included within each of the tables.

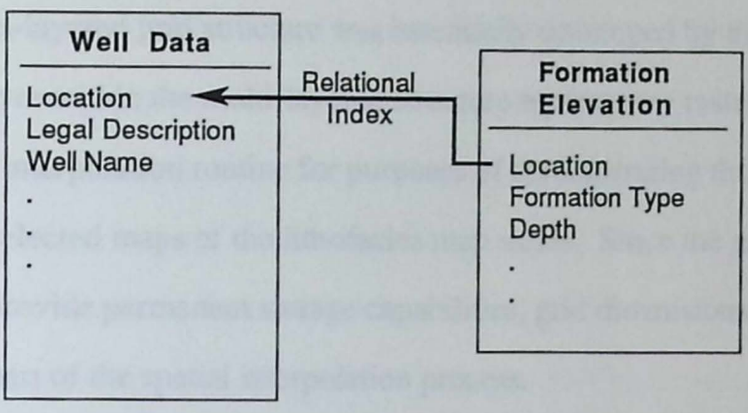

Figure 3.5 - Relational file structure for storage and analysis of the stratigraphic data of the LKC Groups.

Table 3.1 - Field descriptions for the Well Data Table.

Well Data

Field	Type	Description
Location	Integer	File Index, Relational Key
Legal Description	Alpha 14	Well Description based upon Federal Land Survey system.
Well Name	Alpha 30	
KB Elev	Real	Kelly Bushing Elevation
x Coord	Real	X coordinate based upon arbitrary Cartesian coordinate system.
y Coord	Real	Y coordinate based upon arbitrary Cartesian coordinate system.

Table 3.2 - Field descriptions for the Formation Elevation Table.

Well Data

Field	Type	Description
Location	Integer	File Index, Relational Key
Formation	Alpha 15	Stratigraphic Unit Description
Depth	Real	Depth below Kelly Bushing
Datum	Real	Elevation

The multi-layered grid structure was essentially developed by the interpolation routine. Each layer within the multi-layered structure represents a raster or grid image produced by the interpolation routine for purposes of demonstrating the facies distribution for selected maps of the lithofacies map series. Since the grid structure was not intended to provide permanent storage capabilities, grid dimensions were defined dynamically as part of the spatial interpolation process.

Each of the grid layers represents an independent two-dimensional data structure. While all of the two-dimensional grid layers were defined identically for this study, there is no reason that individual layers could not be defined differently to obtain finer or coarser spatial resolution for specific layers. This approach could be used to further simplify individual horizons where less detail is required reducing the overall storage demands and increasing interpolation performance. While the multi-layered grid structure is similar to the voxel structure, no attempt was made to develop a comprehensive spatial index for the overall multi-layered grid structure, thus restricting further geographical analysis of the facies distribution. Since, the focus of this study was to automate reconstruction of the lithofacies map series for display purposes rather than performing geographical analysis, the simple multi-layered grid structure was assumed to be adequate.

The combination of a simple relational structure and multi-layered grid or raster structure is far simpler to implement than either a voxel or a topological structure. The facies distribution presented within a lithofacies map series is defined with two-dimensional maps, which can be displayed effectively using the multi-layered grid based structure. The combination structure offers a more functional capability for separating the interpolation model from data management. Also the combination

structure provides the flexibility to modify interpolation schemes without modifying the underlying data management structure. With this approach, the data can also be managed in the form of simple point data.

Because the multi-layered grid structure is dynamic and will not be preserved beyond individual reconstruction efforts, it will not present the storage and scale limitations presented by a permanent voxel structure. Therefore, the scale, vertical resolution, and horizontal resolution can be determined entirely by the application and the individual that is implementing the reconstruction. This ultimately provides the flexibility required for a more functional reconstruction capability that can be readily adapted not only to different scales for reconstruction of the LKC Groups but also to other geographic applications.

Stratigraphic Analysis

The primary function of stratigraphic analysis is to correlate the well data to a defined vertical stratigraphic datum and then create the appropriate data files to be used as input for the spatial interpolation component of the reconstruction model. In order to correlate the well data for proper map construction, the base of the transgressive carbonate member was defined as a datum. Once the stratigraphic data were correlated to the datum, the slice data required to interpolate the individual lithofacies maps was then identified based upon the vertical position above this datum. For example, the Base+2, Base+4, and Base+6 time-slices represent arbitrary slices that are two, four, and six feet, respectively, above the base of the transgressive carbonate member. Figure 3.6 provides a diagram of the steps required to stratigraphically correlate the well data.

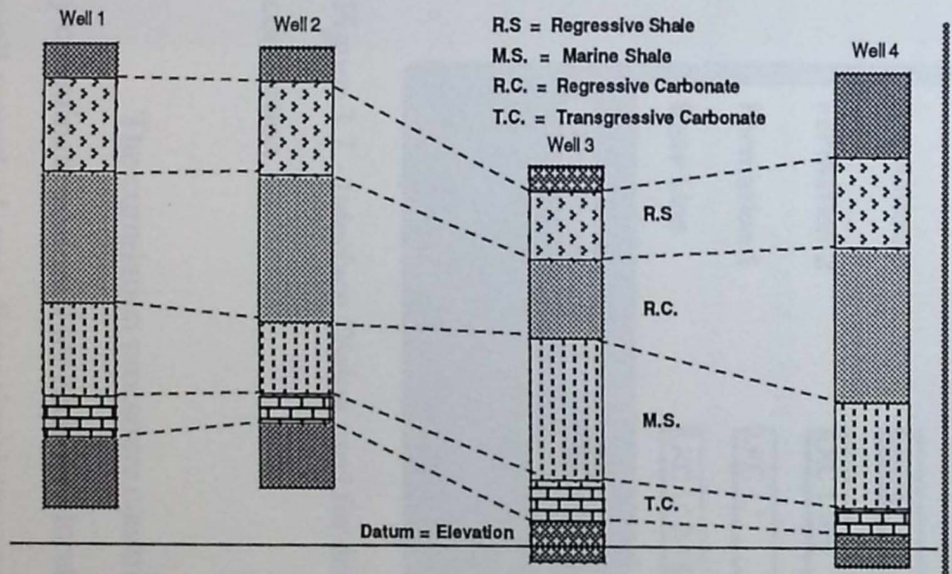

1.) Stratigraphic Section demonstrating well data correlated by elevation.

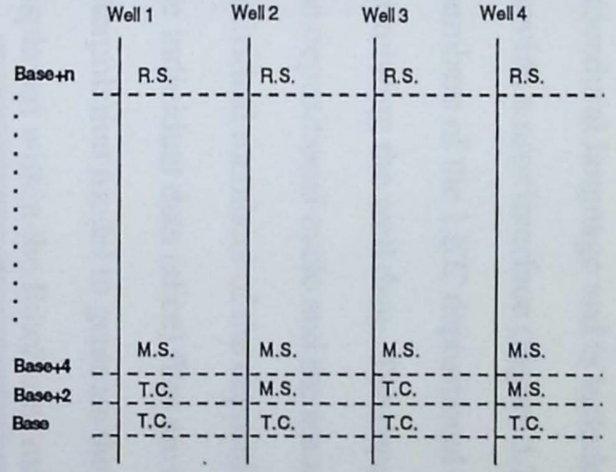

3.) Tabled slice data extracted from correlated well data.

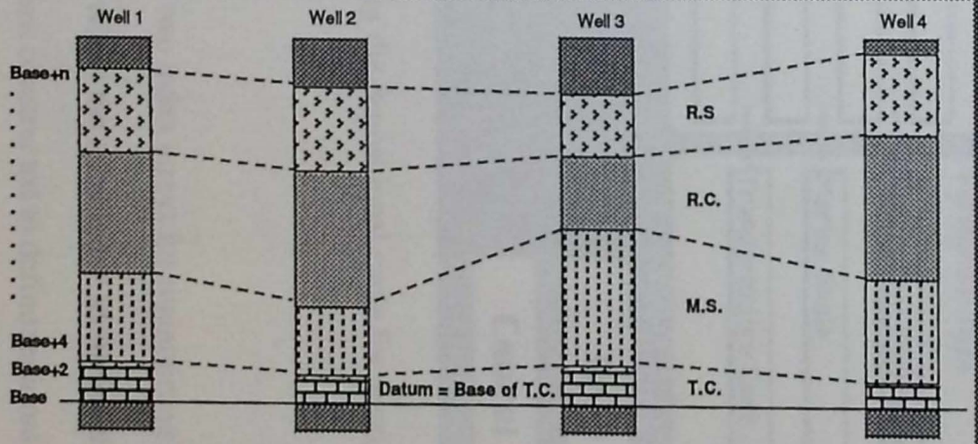

2.) Stratigraphic Section demonstrating well data stratigraphically correlated to the base of the transgressive carbonate member.

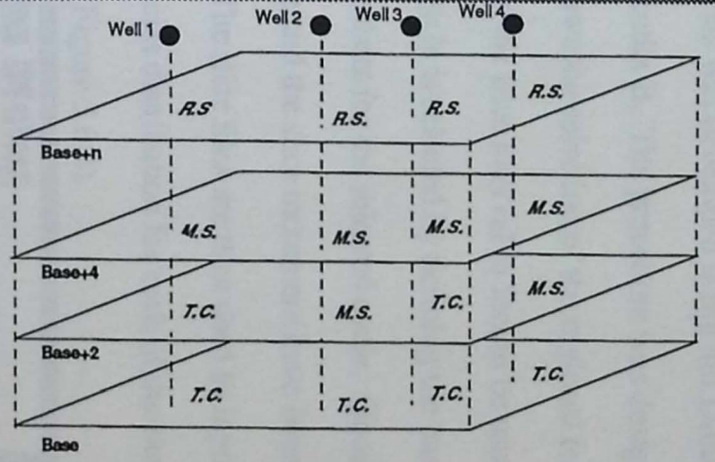

4.) Slice data represented in a temporal map set.

Figure 3.6 - Conceptual model for correlating the vertical stratigraphic sequence of the LKC Groups.

The algorithm for stratigraphic analysis was developed using 4th Dimension's procedural language and is included in Appendix B. The procedure was designed to provide a user interface (Figure 3.7) that allows the selection of the regional formation members of the LKC depositional cycles and the slice interval in feet to be used when correlating the well data. The depositional cycle is selected by defining the base line of the depositional cycle and the associated members for the selected cycle. Once the individual members of the depositional cycle and the slice increment have been defined, the individual data (slice) files are created. The slice files are then used as input to the interpolation model to generate the spatial facies distribution for each of the maps to be displayed within the lithofacies map series (Figure 3.6.4).

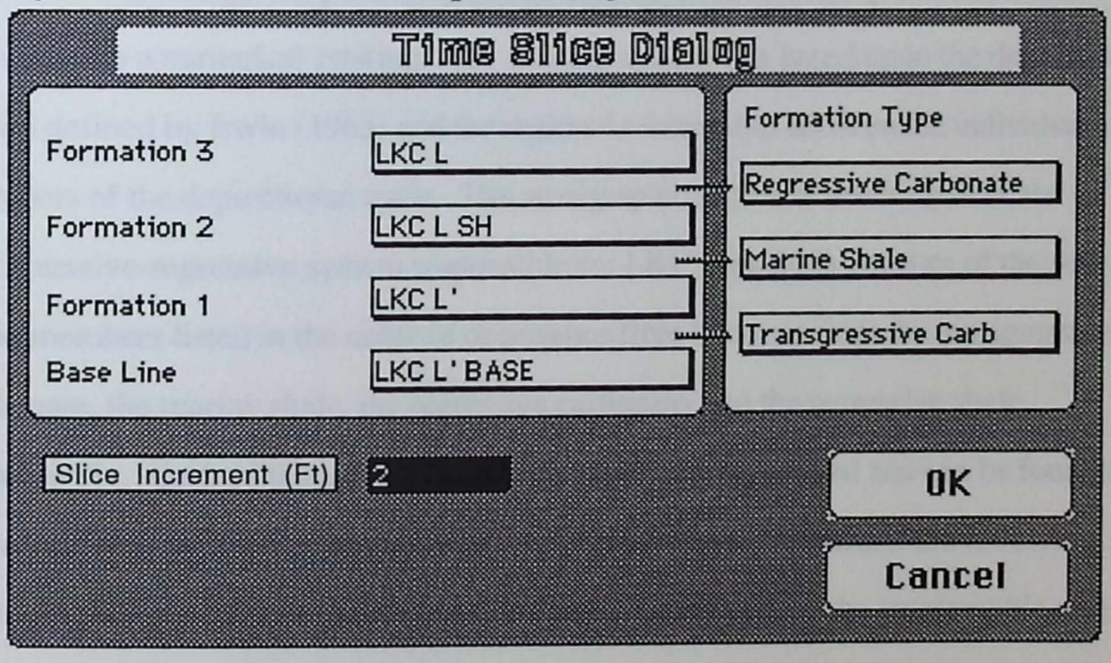

Figure 3.7 - Interface Dialog used for defining the depositional cycle for stratigraphic correlation.

The correlation procedure constructs two index arrays for maintaining the x and y coordinate positions for each well location where the array index identifies the logical well record. A two-dimensional array was then constructed to define regional

stratigraphic development where the first index corresponds to the well location and the second index corresponds to the vertical increment above the datum (i.e. the Base+2, Base+4, etc.). The second index is incremented based upon the vertical increment that was defined through the interface dialog (Figure 3.7). The stratigraphic unit associated with each vertical increment was determined by subtracting the elevation of the base line defined through the interface dialog (Figure 3.7) from the elevation attached to each of the stratigraphic horizons (Figure 3.6.2, and 3.6.3).

In order to create slice files that could be interpolated to demonstrate the facies distribution spatially, the qualitative names attached to the stratigraphic units were converted to a numerical ranking. The ranking system was based upon the depositional model defined by Irwin (1965) and the regional relationship between the individual members of the depositional cycle. The stratigraphic sequence resulting from the transgressive-regressive system responsible for LKC deposition consists of the four basic members listed in the order of occurrence from bottom to top: the transgressive carbonate, the marine shale, the regressive carbonate, and the regressive shale, respectively. Each of these four members is regionally significant and can be found at all locations within the region surrounding the study area. Therefore, the following ordinal ranking system was developed for purposes of defining the stratigraphic units in a manner that would represent the sequence of occurrence within the context of the regional depositional system:

1 = Transgressive Carbonate

2 = Marine Shale

3 = Regressive Carbonate

4 = Regressive Shale

Once the formation rankings were assigned, the individual slice files were constructed for the L zone stratigraphic cycle starting at the Base+4 slice and ending at the Base+22 slice using a 2 foot vertical increment. This corresponds with the paleogeographic reconstruction completed by Bader (1989). This range represents evolution of the system from early in the transgressive phase of deposition through transition to the regressive shale which marks the completion of the depositional cycle.

Spatial Interpolation

The problem with developing an interpolation model lies in the selection of a plausible model that not only suits the data (Burrough, 1986; Jones, 1986) but also provides an adequate means of displaying the data (MacEachren, et. al. 1991). The individual lithofacies maps produced as part of the lithofacies map series represent a form of a dasymetric map that essentially portray a discrete surface similar to that of a choropleth map. The primary distinction between the choropleth map and the dasymetric map lies in the selection of boundaries used to portray the data; the choropleth map generally utilizes administrative boundaries, while the dasymetric map utilizes boundaries defined by the data (Campbell, 1984).

While the discrete interpolation methods may appear to provide the appropriate form of output to create the lithofacies maps, discrete interpolation operators generally assume that the control points are not spatially related. This presents a problem when trying to estimate the form of a surface where control points are spatially related as is the case with the stratigraphic data used to generate the lithofacies maps. An example of the problems of utilizing a discrete algorithm, such as Thiessen polygons, for

developing the lithofacies maps is presented in Figure 3.8 where the system is assumed to posses an ordered stratigraphic sequence.

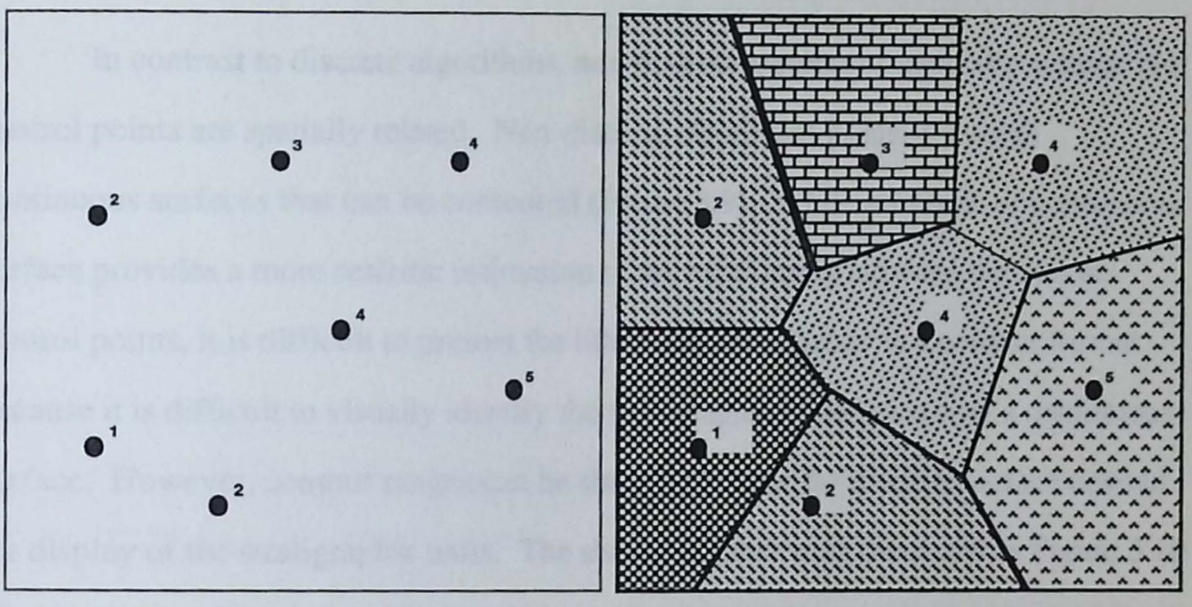

1. - Ordinal well data from a representative time-step file identifying the stratigraphic development for individual well sites.

2. - Ordinal surface developed using Thiessen polygons.

Figure 3.8 - Interpolation of a lithofacies map using Thiessen polygon techniques.

Thiessen polygons are created by sub-dividing a region into individual areas based upon the configuration of the data points (Burrough, 1986). The extent of each region is defined by bi-secting the mid-points between nearest neighbor pairs and extending the bi-sectors until they intersect to create individual polygons (Rhynsberger, 1973). The value assigned to each of the individual polygons is obtained from the nearest data point used to define the polygon, which creates a discrete or stepped surface (Figure 3.8).

From Figure 3.8 it is obvious that discrete interpolation algorithms do not provide an effective means of presenting the distribution of the stratigraphic units. The ordered stratigraphic sequence from 1 to 5 is ignored by placing non-adjacent

stratigraphic members in sequence on the map (i.e. regions of stratigraphic types 2 and 4, 1 and 4, or 2 and 5)

In contrast to discrete algorithms, non-discrete algorithms generally assume that control points are spatially related. Non-discrete algorithms produce smooth continuous surfaces that can be contoured (Figure 3.9). While a smooth or continuous surface provides a more realistic estimation of the relationship between the various control points, it is difficult to present the lithofacies distribution in a contour format because it is difficult to visually identify the stratigraphic boundaries over a continuous surface. However, contour ranges can be shaded to create the discrete surface desired for display of the stratigraphic units. The shaded contour map presented in Figure 3.10 clearly presents the stratigraphic distribution in a discrete dasymetric map form while maintaining the order of the stratigraphic sequence imposed by the depositional system.

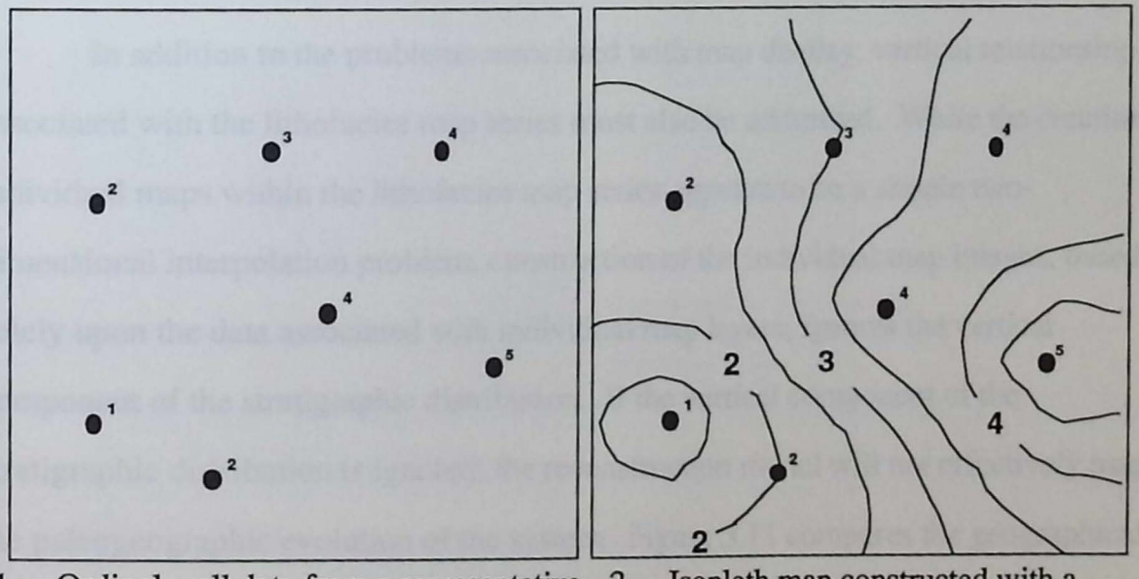

1. - Ordinal well data from a representative time-step file identifying the stratigraphic development for individual well sites.

2. - Isopleth map constructed with a weighted average interpolation technique (MacGRIDZO Ver. 3.3, RockWare, Inc., 1991) .

Figure 3.9 - Interpolation of well data using a weighted average technique. Contours were developed with a commercial package.

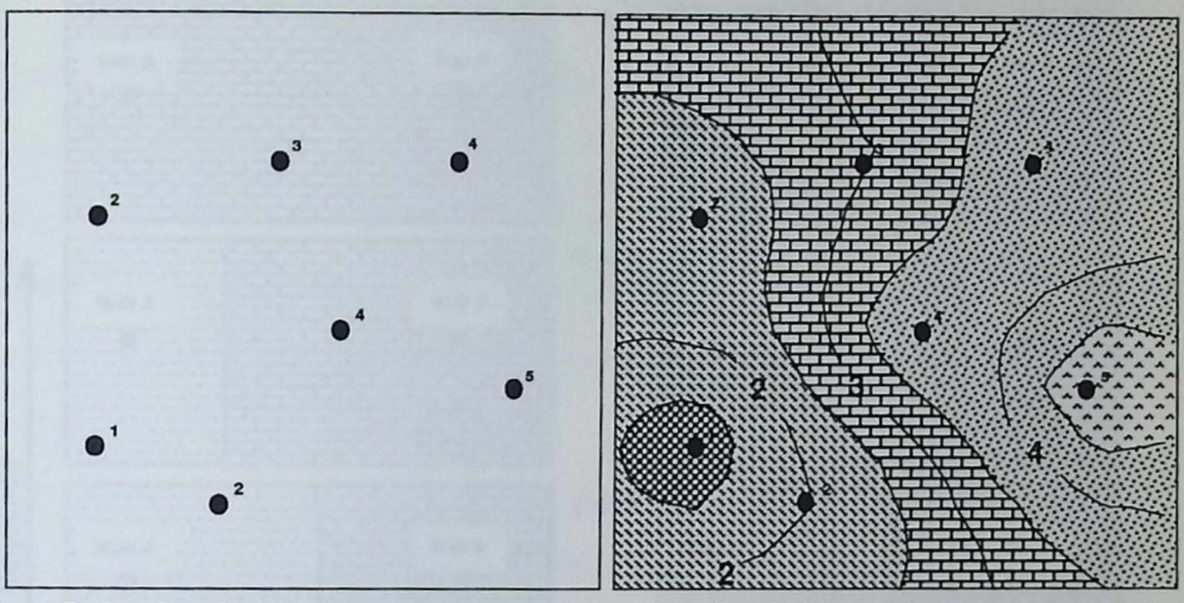

1. - Ordinal well data from a representative time-step file identifying the stratigraphic development for individual well sites.

2. - Shaded isopleth map constructed with a weighted average interpolation technique (MacGRIDZO Ver. 3.3, RockWare, Inc., 1991) .

Figure 3.10 - Shaded isopleth map constructed using a weighted average interpolation technique.

In addition to the problems associated with map display, vertical relationships associated with the lithofacies map series must also be addressed. While the creation of individual maps within the lithofacies map series appears to be a simple two-dimensional interpolation problem, construction of the individual map images, based solely upon the data associated with individual map layers, ignores the vertical component of the stratigraphic distribution. If the vertical component of the stratigraphic distribution is ignored, the reconstruction model will not effectively map the paleogeographic evolution of the system. Figure 3.11 compares the geographical representation of the migration of the stratigraphic boundaries between two wells where individual map slices are constructed using three-dimensional versus a more generic two-dimensional interpolation approach (Figure 3.11.2).

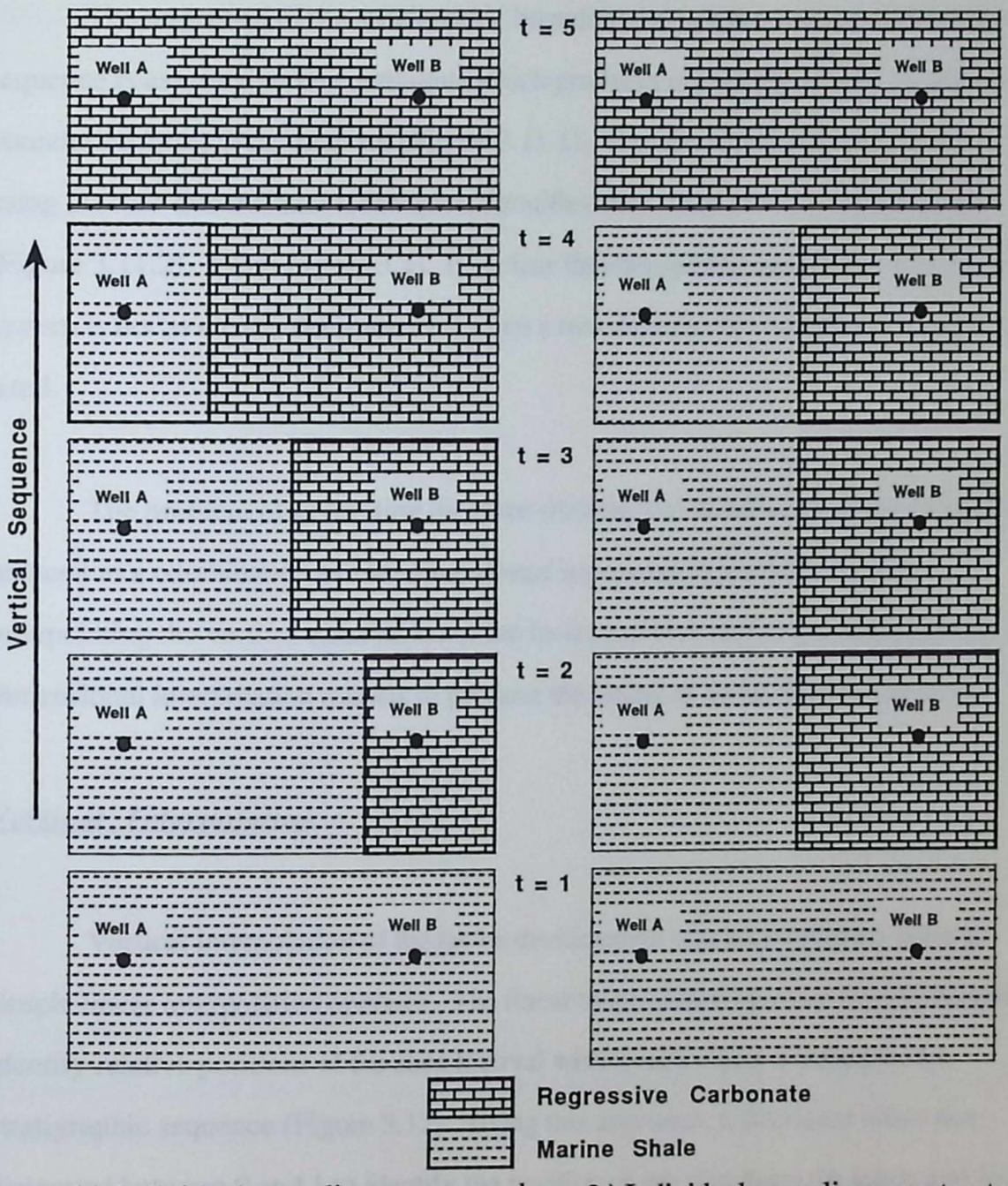

1.) Individual map slices constructed where stratigraphic boundary is interpolated from current layer and adjacent layers.
(three-dimensional perspective)

2.) Individual map slices constructed where stratigraphic boundary is interpolated from current layer only.
(two-dimensional perspective)

Figure 3.11 - Reconstruction of a stratigraphic system comparing migration of stratigraphic boundaries between map slices using three-dimensional versus two-dimensional construction techniques.

The migration of the stratigraphic boundary through the vertical stratigraphic sequence is assumed to be continuous which produces a gradational shift of the facies boundaries through the map set (Figure 3.11.1). The lithofacies map set generated, using the two-dimensional techniques, identifies very sharp static facies boundaries (Figure 3.11.2). From Figure 3.11, it is clear that the paleogeographic evolution of the system is not as clearly demonstrated when a two-dimensional interpolation process is used.

The problem of generating the three-dimensional distribution of the facies was reduced to a combination of two-dimensional interpolation problems by first interpolating the vertical distribution of the facies and then applying traditional two-dimensional interpolation models to produce the lateral or aerial distribution maps.

Vertical Interpolation

Vertical interpolation of the facies development was accomplished using a simple linear interpolation operator. The linear interpolation operator was developed to identify relative positions of the slice interval within each of the members in the stratigraphic sequence (Figure 3.12). Using this approach, a fractional value was generated between 0 and 1 to identify the position of the slice from the upper and lower facies boundaries. The decimal fraction resulting from the interpolation was then added to the ordinal ranking factor to provide a vertically interpolated rank with the integer portion identifying the formation type and the decimal portion identifying the relative position from the respective stratigraphic boundaries. Basically, the interpolated rank provides a simple mechanism for identifying the relative position of the stratigraphic boundary from individual wells on a map. The vertical interpolation procedure was

developed using FORTRAN and is included in Appendix B. Both the ordinally ranked slice data files and the associated vertically ranked slice data files are included in Appendix C.

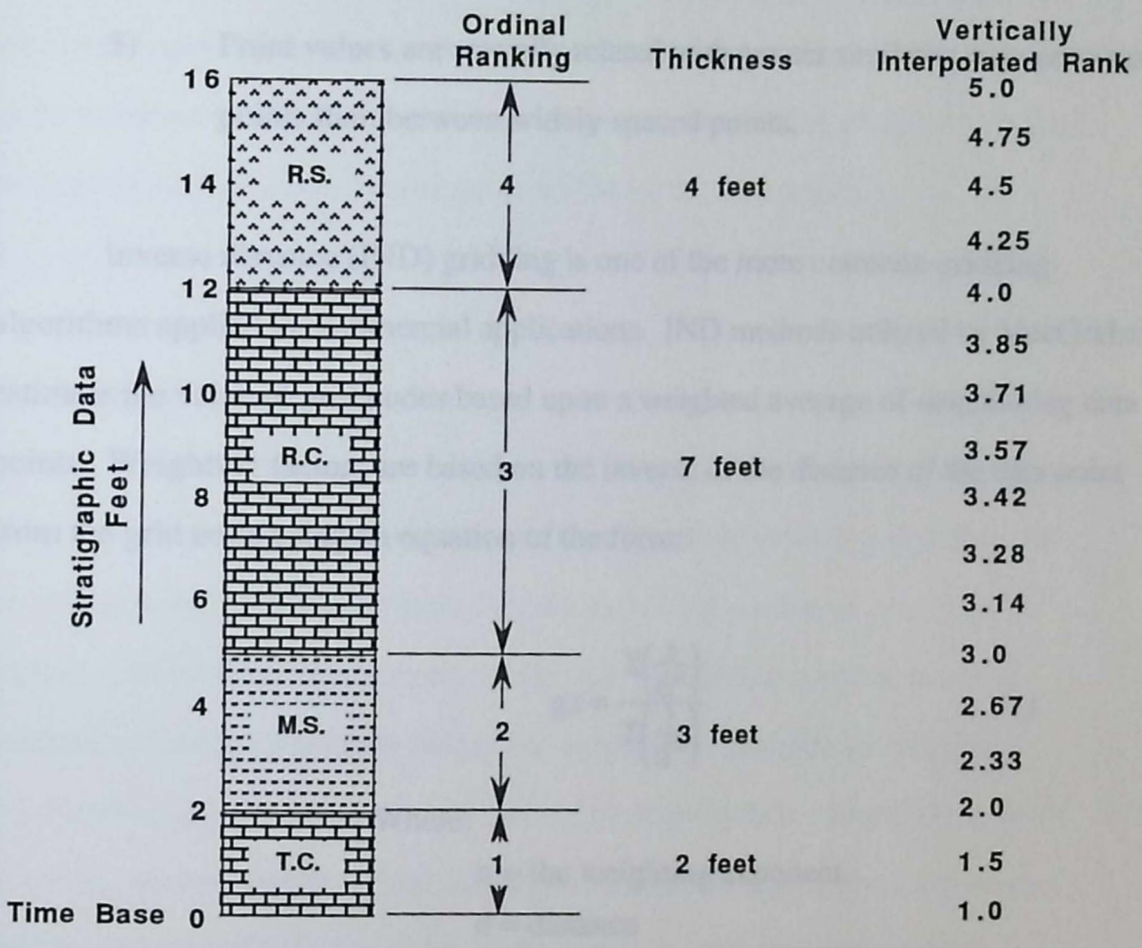

Figure 3.12 - Linear interpolation of well data to identify the vertical distribution of the facies development.

Surface Interpolation

Once the slice files were modified to include the vertically interpolated ranks, a mathematical grid was constructed from each of the slice files using MacGridzo version 3.3. MacGridzo, which was developed by Rockware, supports two standard gridding

options: Inverse Distance and Weighted Least Squares. Both gridding methods are based upon the following assumptions:

1) Control points are single-valued and unique.
2) The surface is continuous between all observation points.
3) Point values are spatially related with greater similarity between nearby points than between widely spaced points.

Inverse distance (IND) gridding is one of the more common gridding algorithms applied in commercial applications. IND methods utilized by MacGridzo estimate the value of grid nodes based upon a weighted average of neighboring data points. Weighting factors are based on the inverse of the distance of the data point from the grid node using an equation of the form:

$$gz = \frac{\Sigma\left(\frac{z}{d^n}\right)}{\Sigma\left(\frac{1}{d^n}\right)} \qquad (1)$$

Where:

n = the weighting exponent.
d = distance
gz = grid node to be calculated
z = data point value

The grid produced with IND gridding provides a smooth and continuous surface with values that are not extrapolated beyond the range of data points. This basically renders a grid in which the range of grid values is smaller than the data point range (i.e. the smallest grid value is greater than the minimum data point, and the largest grid value is less than the maximum data point).

The "Weighted Least Squares" (WLS) gridding method used by MacGridzo is more commonly known as "Moving Weighted Least Squares". This type of gridding method is similar to that of the IND methods; however, the weighted z values that are produced through equation (1) are then used to compute a first order polynomial to represent a plane in space for each grid node. The intersection of the grid node with the plane determines the actual grid node value. As a result, the grided values more accurately represent the data range provided by the data points.

Gridding Parameters

Both gridding methods supported by MacGridzo can be adjusted with several gridding parameters including the number of control points, search pattern, and weighting exponents. Although MacGridzo supports up to 40 control points for generating grid nodes using either gridding method, the documentation suggests a typical value of 5 control points. With both types of gridding, the number of control points determines the degree of averaging that will be performed over the entire surface. Fewer control points produce surfaces in which grid values are more strongly influenced by nearby points. Adding control points tends to reduce the effect of local control points and produces more of an averaging or smoothing effect for the gridded surface.

When selecting control points, MacGridzo defaults to the nearest control points for determining grid values; unfortunately, this can lead to problems when data points are clustered. Clustered data points can lead to a uni-directional search pattern that essentially leaves the resulting estimate

unconstrained or directionally biased (Davis, 1986). Directional search capabilities provide the utility to make grid node estimates reflect a more evenly distributed sample of control points about a grid node (Figure 3.13). Davis (1986) outlined different types of radial search patterns including both the quadrant and octant methods where control points are evenly distributed over each quadrant or octant surrounding the grid node. MacGridzo provides a directional or radial search option to accommodate clustered data, but the MacGridzo documentation does not specify which type of radial search is performed when developing a grid.

The weighting exponent is used to specify the influence control points have with increasing distance from a grid node. Individual data points are weighted according to the inverse of the distance between the grid node and the data point. Raising the exponent in the denominator of the inverse distance equation (1) reduces the influence exerted by distant points. Therefore, the greater the exponent, the less distant data points will influence the value generated for the grid cell. The MacGridzo documentation suggests a range of between 2.0 and 3.0 to obtain the best results; however, this ultimately is dictated by the application.

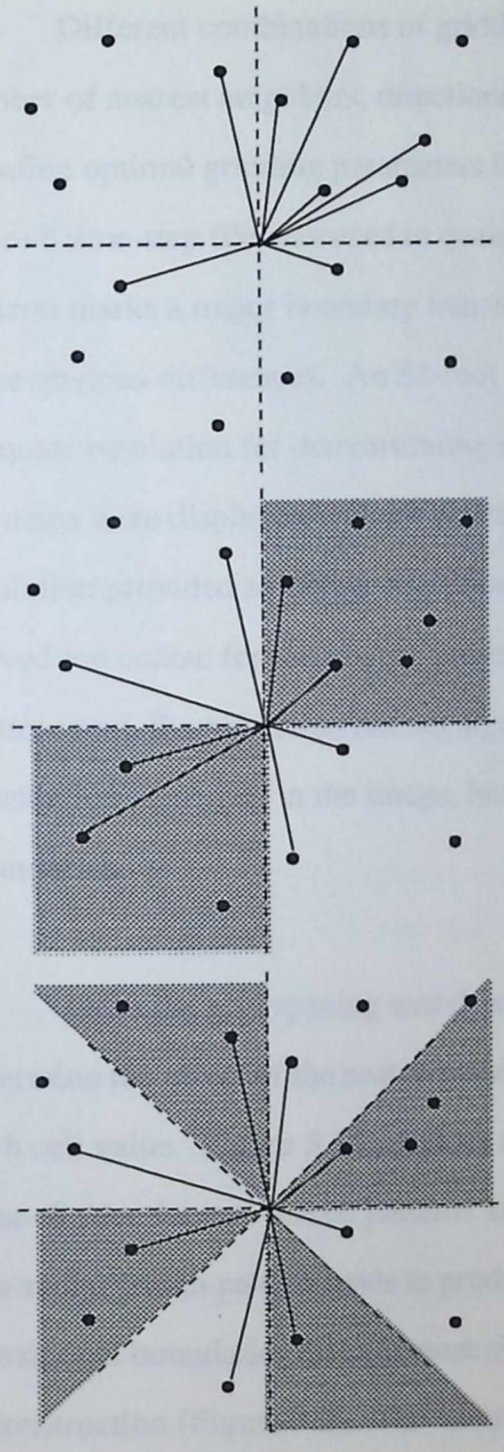

a). Nearest neighbor search technique with no radial constraints. Locates n nearest neighbors around grid node.

b). Quadrant search pattern forces an equitable sampling of points in each of the four quadrants surrounding the grid node.

c). Octant search pattern forces an equitable sampling of points in each of the eight octants surrounding the grid node.

Figure 3.13 - Search patterns for selecting nearest neighbor control points.

(modified from Davis, 1986, Fig. 5.57 pg 374.)

Different combinations of gridding parameters including grid cell resolution, number of nearest neighbors, directional search, and weighting factors were examined to define optimal gridding parameters for generating the lithofacies images. The Base+8 time-step file was used to evaluate various gridding parameters because this horizon marks a major boundary transition where variations in gridding will produce more obvious differences. An 82-foot grid spacing was selected because it provided adequate resolution for demonstrating stratigraphic distribution for the scale at which the maps were displayed without generating a significant storage overhead. A finer resolution provided smoother transitional boundary lines while a coarser resolution proved too coarse for the images presented in the lithofacies map series (Figure 3.14). In any event, the resolution did not significantly effect the overall stratigraphic distribution presented in the image, but rather just the quality and smoothness of the boundaries.

Once the grid spacing was determined, search parameters were varied to determine the effect of the search patterns and the number of points used to generate each cell value. Figure 3.15 provides a summary of the variation produced within the Base+8 slice for two search patterns and variation in number of nearest neighbors. The non-radial search pattern tends to produce a more conservative image with smoother transitional boundaries that are more similar to boundaries produced by hand reconstruction (Figure 3.2). The variability introduced by changing the number of nearest neighbors used in calculation of individual cell values did not produce significant variation in the output image.

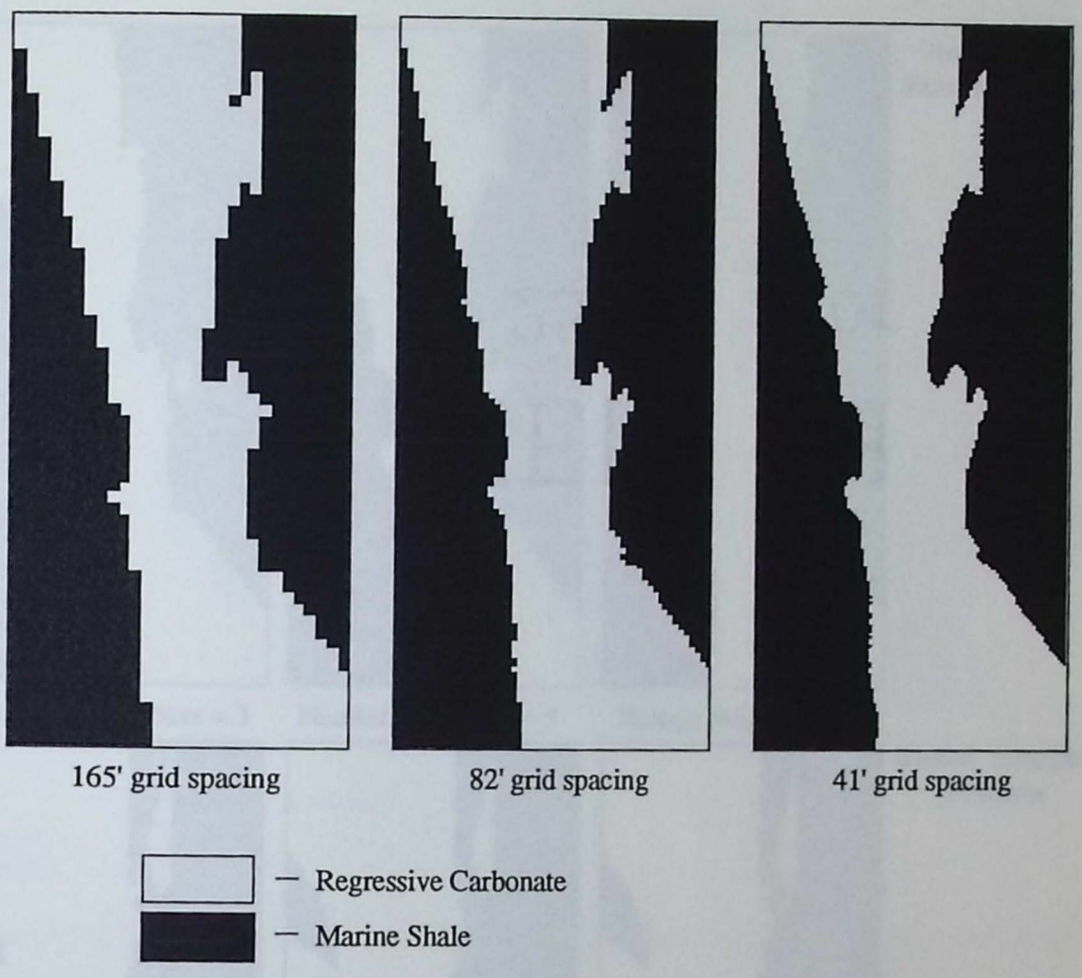

Figure 3.14 - Comparison of variation in grid spacing on image construction for the Base+8 slice of the Triangle field L zone lithofacies map series.

Weighting factors also were examined to determine their impact upon image construction. Figure 3.16 identifies the effects produced by a variation in the weighting factors through a range from 2.0 to 3.5 which is consistent with the range recommended within the MacGridzo documentation. Again, the variation produced within the image from changes in the weighting factor was not very significant.

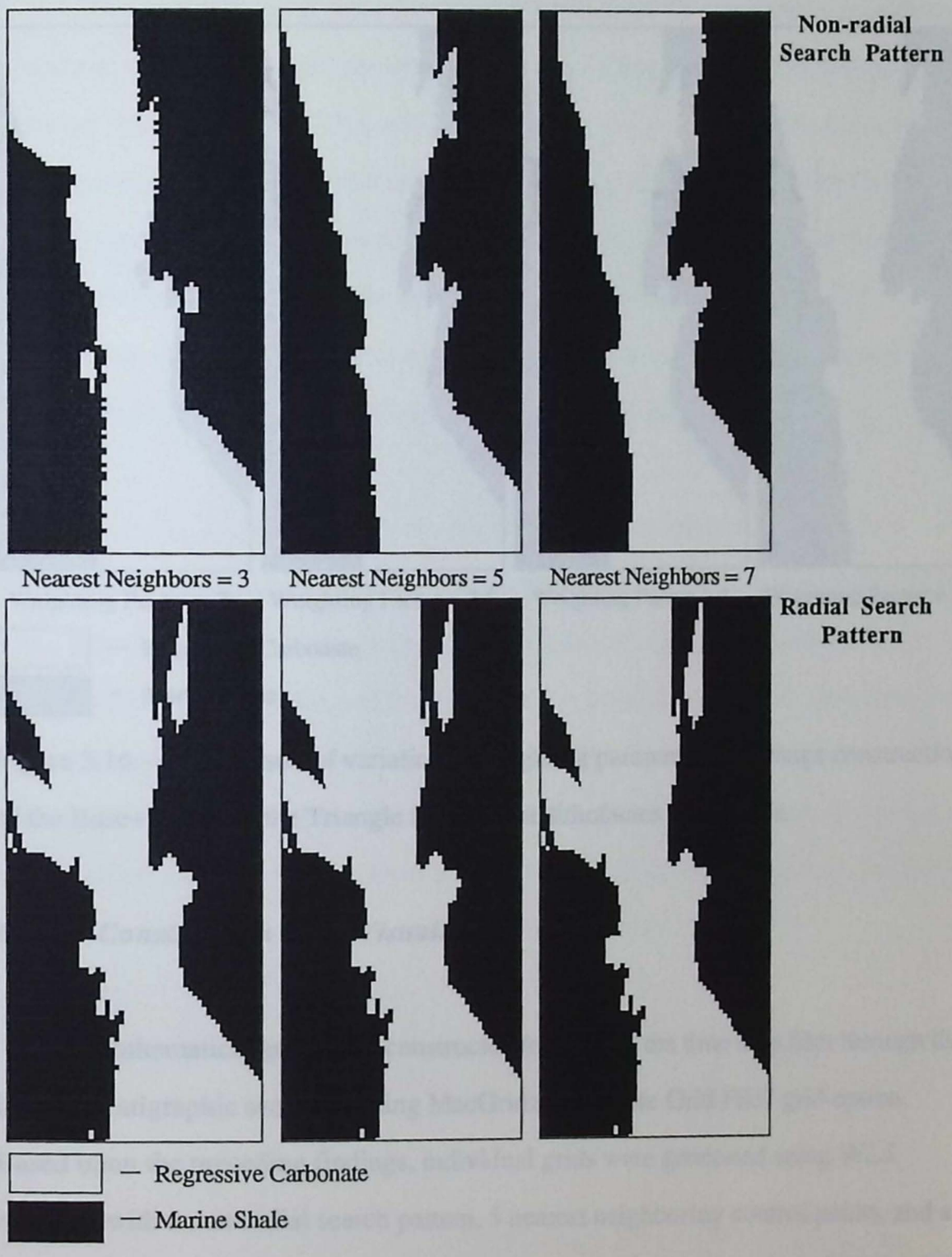

Figure 3.15 - Comparison of variation in search pattern and number of nearest points used for image construction of the Base+8 slice of the Triangle field L zone lithofacies map series.

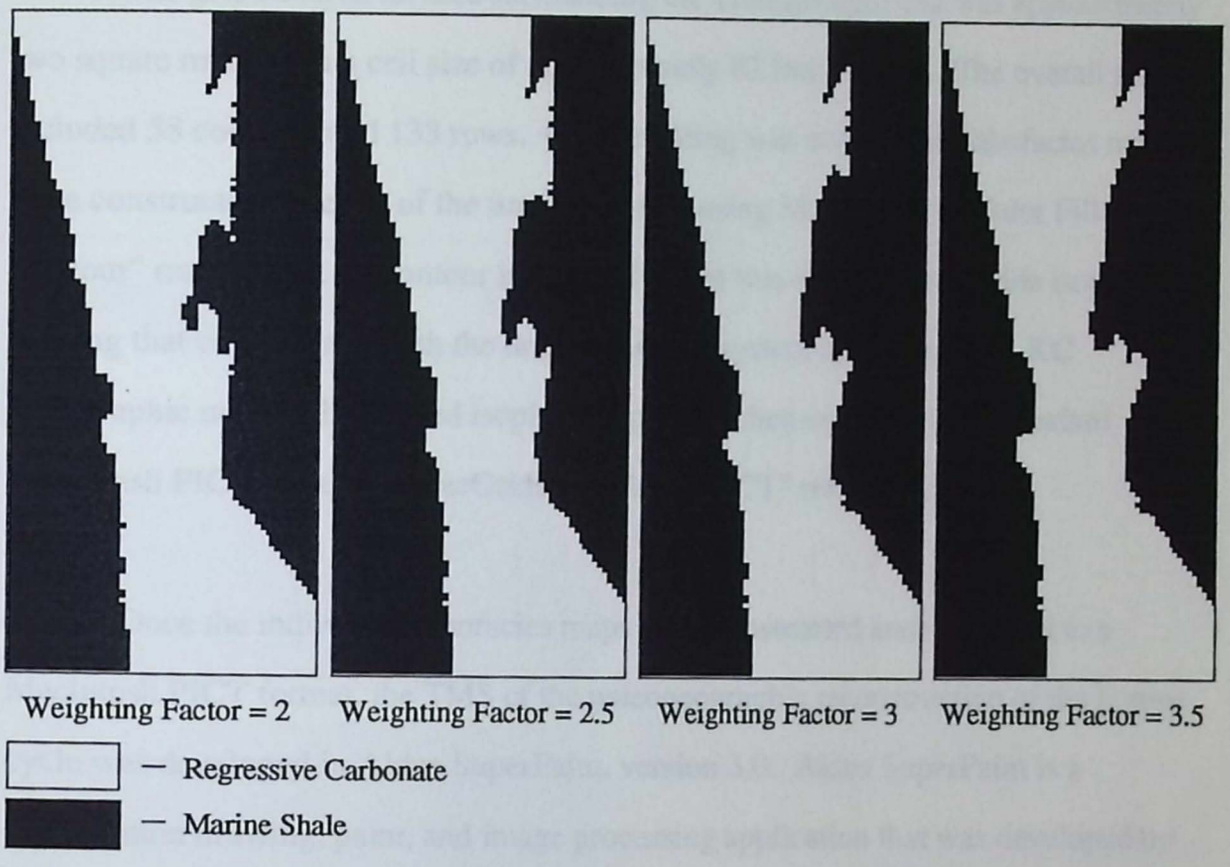

Figure 3.16 - Comparison of variation in weighting parameters for image construction of the Base+8 slice of the Triangle field L zone lithofacies map series.

Image Construction and Visualization

Mathematical grids were constructed for each of the time-step files through the L zone stratigraphic sequence using MacGridzo's "Create Grid File" grid option. Based upon the preceding findings, individual grids were generated using WLS methods with a non-radial search pattern, 5 nearest neighboring control points, and a distance weighting factor of 3.0. This combination of gridding parameters was selected because the images produced with this combination provided the greatest similarity to the images constructed manually by Bader (1989).

The grid covered an area surrounding the Triangle field and was approximately two square miles with a cell size of approximately 82 feet per side. The overall grid included 58 columns and 133 rows. Once gridding was completed, lithofacies maps were constructed for each of the time-step grids using MacGridzo's "Color Fill Contour" map option. A contour interval of 1 foot was selected to provide isopleth shading that corresponds with the ordinal ranking system applied to the LKC stratigraphic units. The shaded isopleth maps were then converted to a standard Macintosh PICT file using MacGridzo's "Plot to PICT" reformat option.

Once the individual lithofacies maps were constructed and converted to a Macintosh PICT format, the TMS of the paleogeographic reconstruction of the L zone cycle was developed in Aldus SuperPaint, version 3.0. Aldus SuperPaint is a combination drawing, paint, and image processing application that was developed by Silicon Beach Software. In order to prepare the TMS, the individual lithofacies PICT files were imported into Aldus SuperPaint where appropriate fill patterns were assigned to the shaded isopleth regions. Once edited, the lithofacies maps were arranged in the appropriate temporal sequence and labeled (Figure 3.17).

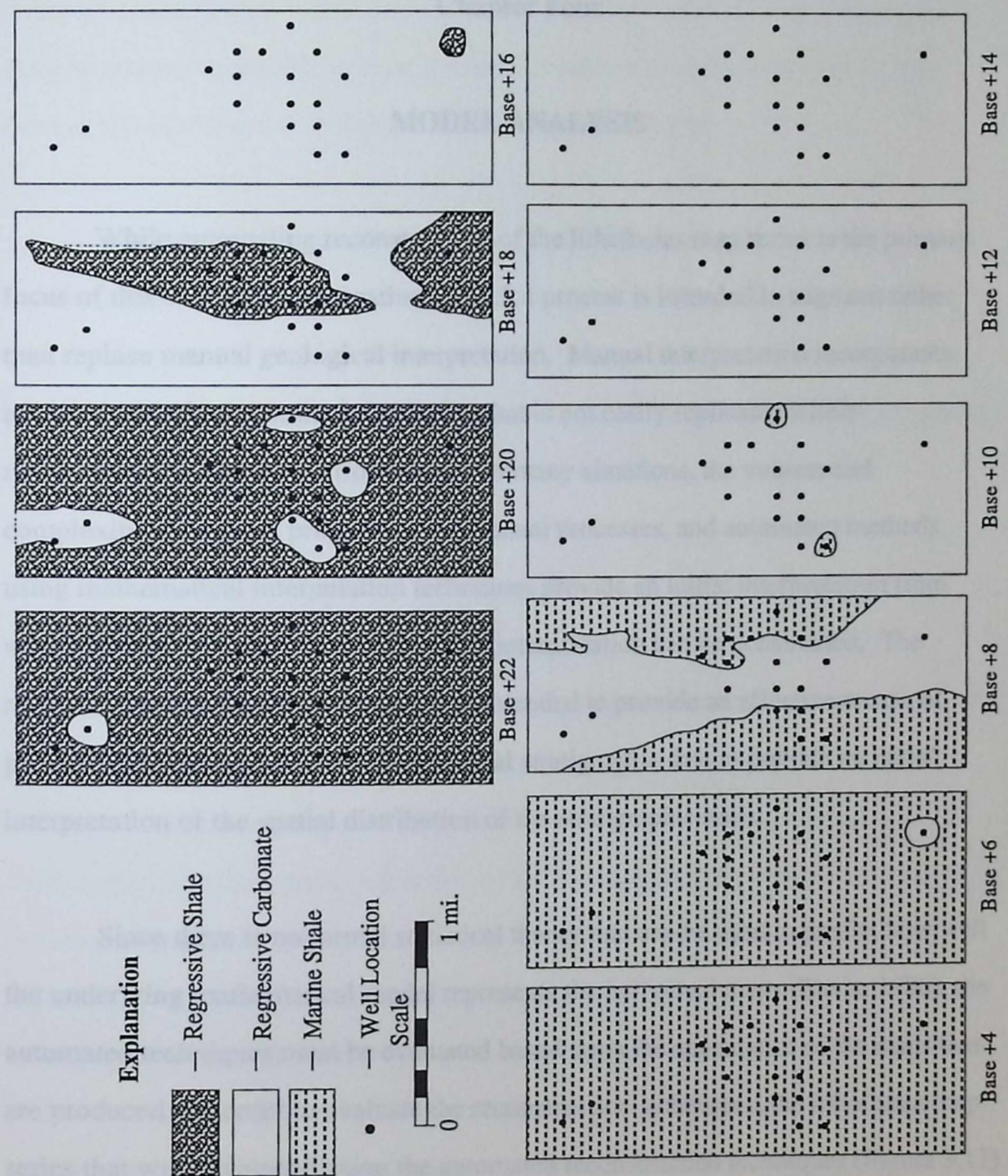

Figure 3.17 - Paleogeographic reconstruction of the Lansing-Kansas City L zone cycle in the vicinity of the Triangle Field using automated reconstruction techniques. Maps are based upon a stratigraphic sequence that is correlated to the base of the transgressive carbonate member (i.e. Base+4 represents the stratigraphic horizon that is 4 feet above the base of the transgressive carbonate member).

Chapter Four

MODEL ANALYSIS

While automating reconstruction of the lithofacies map series is the primary focus of this study, the automation of such a process is intended to augment rather than replace manual geological interpretation. Manual interpretation incorporates intuitive and often abstract information that is not easily replicated within mathematical methods. Unfortunately, in many situations, the volume and complexity of data are prohibitive for manual processes, and automated methods using mathematical interpolation techniques provide an initial interpretation from which a more comprehensive subjective interpretation can be constructed. The reconstruction techniques are therefore intended to provide an effective means of processing the complex three-dimensional stratigraphic data to provide an initial interpretation of the spatial distribution of the stratigraphic units.

Since there is no formal statistical theory that can be used to predict how well the underlying mathematical model represents the individual maps (Davis, 1986), the automated techniques must be evaluated based upon the appearance of the maps that are produced. In order to evaluate the reconstruction techniques, the lithofacies map series that was developed using the automated reconstruction techniques (Figure 3.17) was compared with the lithofacies map series developed manually (Figure 3.2) by Bader (1989). The manual interpretation developed by Bader (1989) provides a basis for evaluation of the automated techniques because this subjective interpretation was developed from the underlying conceptual model. This comparison should be used to determine the degree to which the automated techniques adhere to the rules of the

underlying conceptual model rather than the degree to which the map images match those produced manually because the manual interpretation includes a subjective component that was not included in the mathematical model.

The system continuity, temporal evolution, and regional geological trend are the three primary factors that control the geographic configuration and evolution of the paleogeographic regions within the LKC system. The lithofacies map series constructed with the automated techniques will be reviewed in the context of each of these controlling factors.

System Continuity

There are four basic members of the regional stratigraphic sequence associated with the depositional cycles of the LKC Groups, and these were defined to occur in the following ordered sequence from bottom to top: transgressive carbonate, marine shale, regressive carbonate, regressive shale. The sequence was controlled by the regional depositional system, and all four members are represented in the L zone cycle in the study area. The ordinal ranking system that was designed to identify the stratigraphic sequence provided the necessary capabilities for maintaining the system continuity. When comparing both lithofacies map series, the map series constructed with the automated techniques (Figure 3.17) provides a clear and ordered sequence of stratigraphic members that conforms to that presented by Bader (1989) (Figure 3.2).

Temporal Evolution

Temporal evolution is inferred from the vertical stratigraphic sequence, and it is presented within the paleogeographic map series by the migration of stratigraphic boundaries. The vertical ranking procedure that was implemented was intended to influence the position of stratigraphic boundaries presented in map form based upon the position of the slice horizon within the vertical extent of the stratigraphic member (Figure 3.12). Upon reviewing the lithofacies map series (Figure 3.17), it is apparent that this approach produced somewhat mixed results. Overall the automated techniques did identify a temporal evolution that was consistent with the underlying depositional model. However, there are basic differences between the automated interpretation and the manual interpretation that need to discussed further.

The primary distinction between the manually produced map series and the automated map series lies in the evolution of the migration of stratigraphic boundaries. This is particularly evident in the maps that identify the transitional phases of the depositional cycle where deposition is changing from one stratigraphic member to another in response to changing depositional conditions. These transitional phases occur between each of the stratigraphic members in the depositional cycle. The sequence from the Base+06 through the Base+12 identifies the transition from deposition of the marine shale to the regressive carbonate while the sequence from the Base+16 through the Base+20 identifies the transition between the regressive carbonate and the regressive shale (Figures 3.2 and 3.17).

By examining the sequence from the Base+06 through the Base+12, the differences between the manual interpretation and the automated interpretation can be

better defined (Figure 4.1). The automated techniques produced a much more abrupt stratigraphic boundary evolution which did not extend into the Base+12 slice as did the manual interpretation. The Base+08 slice within the automated sequence demonstrated a much greater level of integration than the comparable slice in the manual sequence, but the most striking difference between the two map series is demonstrated by the Base+10 and the Base+12 slices. Within the Base+10 slice of the automated sequence, the transition was nearly complete with only isolated areas around two control points having marine shale. In contrast, in the manual sequence there was still a significant distribution of the marine shale identified in the Base+10 slice. The Base+12 slice of the manual sequence identifies some marine shale even though the marine shale is not represented by any of the data points while the automated sequence identifies no marine shale within this horizon. These differences can be attributed primarily to the inability of the interpolation techniques to extrapolate beyond the range of the data identified in the two-dimensional slice.

In summary, the paleogeographic evolution presented using the automated reconstruction techniques was noticeably different from that presented in the manual reconstruction. While the evolutionary relationships identified by the automated techniques are somewhat different from those identified by the manual reconstruction, they are consistent with the evolution defined by the conceptual model (Irwin, 1965; Watney 1980; and Bader 1989).

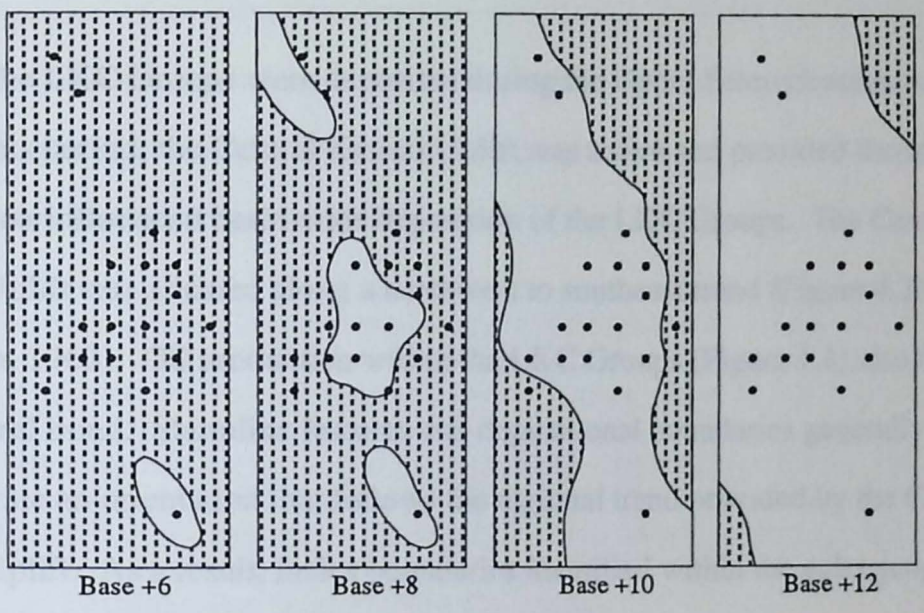

a.) Manual Construction

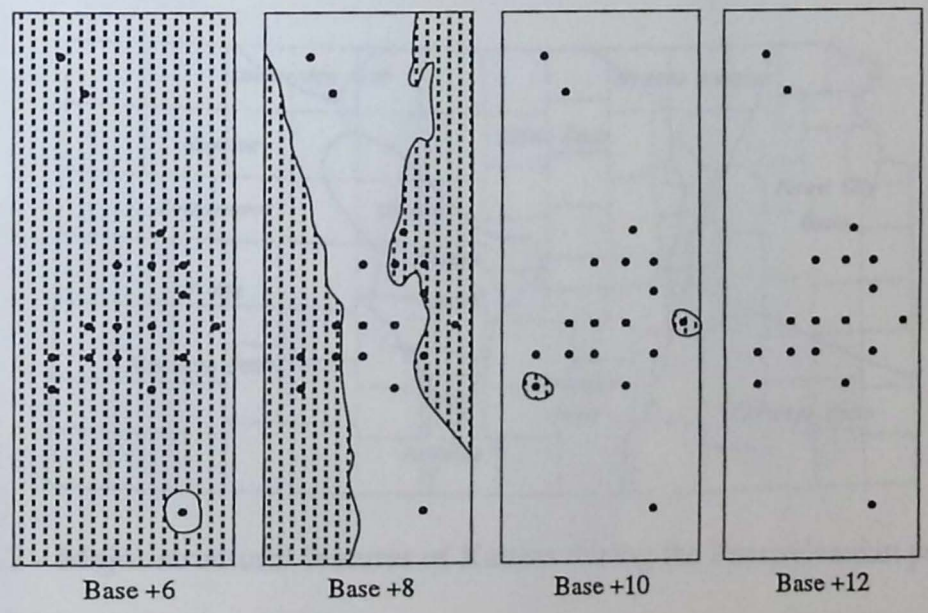

b.) Automated Construction

Figure 4.1 - Comparison of the temporal evolution developed manually with the automated reconstruction for the TMS sequence from the Base+06 through the Base+12 slice intervals.

Regional Trend

The LKC Groups were deposited during the Upper Pennsylvanian period. During this period, the Central Kansas Uplift was active and provided the structural control that influenced basin-wide deposition of the LKC Groups. The Central Kansas Uplift was situated along a northwest to southeast trend (Figure 4.2) (Merriam, 1963). Oil production within the LKC Groups (Figure 1.1) also follows this general trend. Shoreline features and depositional boundaries generally demonstrate an orientation that follows the regional trend provided by the Central Kansas Uplift. As a result, facies boundaries identified within the paleogeographic map series should also demonstrate a similar orientation.

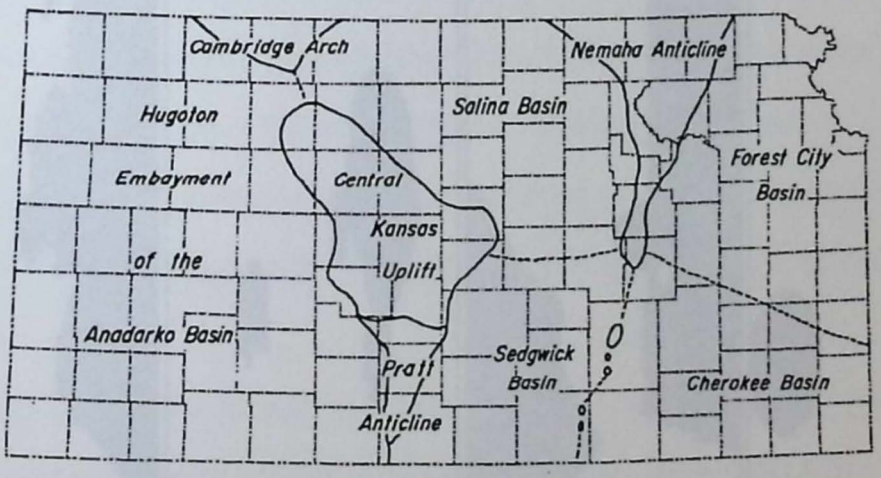

Figure 4.2 - Major structural features of Kansas during the Pennsylvanian period (modified from Merriam, 1963).

The reconstruction techniques use a simple mathematical relationship based upon nearest neighbors, and there is clearly no mechanism in the mathematical model to manage regional trend and relationships that are inferred from this regional geological knowledge. This becomes obvious when evaluating the reconstruction of

the Triangle field. The automated reconstruction appears to maintain the trend similar to that identified within the hand reconstruction where the trend was developed from a geological knowledge base. However, this is merely an artifact of clustering of the data points associated with a mature drilling program within a mature area where available well control has already delineated the regional trend.

The trend associated with the stratigraphic boundaries is best observed in transitional layers, such as the Base+08 slice. When a series of points are randomly removed from Base+08 slice of the Triangle field data set (Figure 4.3), the images produced with the reconstruction techniques did not adhere to the regional trend from northwest to southeast that is inherent to the system.

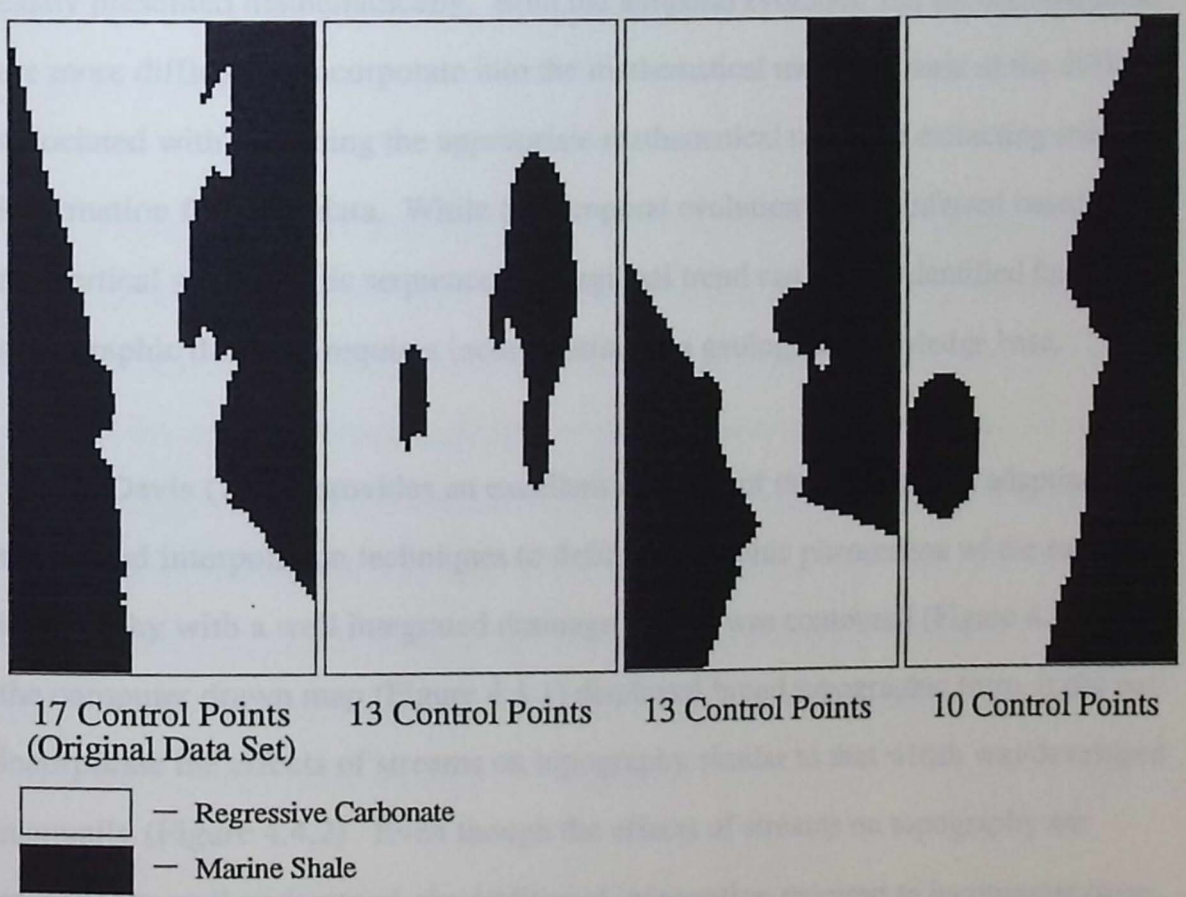

Figure 4.3 - Construction of the Base+08 slice of the Triangle Field L zone lithofacies map series using randomly selected control points.

Model Utility

The utility of the automated reconstruction techniques can not be evaluated based solely upon the degree to which the maps produced by these techniques conform with the manually produced maps. The reconstruction techniques that were developed represent a quantitative effort to present lithofacies relationships within the subsurface environment. The techniques demonstrated here use simple mathematical methods to identify these relationships. While certain components of the system, such as the stratigraphic continuity, can be represented effectively through mathematical methods, many of the relationships within the subsurface can not be easily presented mathematically. Both the temporal evolution and the regional trend are more difficult to incorporate into the mathematical model because of the difficulty associated with designing the appropriate mathematical rules and extracting relevant information from the data. While the temporal evolution can be inferred based upon the vertical stratigraphic sequence, the regional trend can not be identified from the stratigraphic data and requires incorporation of a geological knowledge base.

Davis (1986) provides an excellent example of the difficulty of adapting automated interpolation techniques to define geographic phenomena where surface topography with a well integrated drainage system was contoured (Figure 4.4). While the computer drawn map (Figure 4.4.1) displayed broad topographic form, it did not incorporate the effects of streams on topography similar to that which was developed manually (Figure 4.4.2). Even though the effects of streams on topography are reasonably well understood, the additional information required to incorporate these effects is not available from the data.

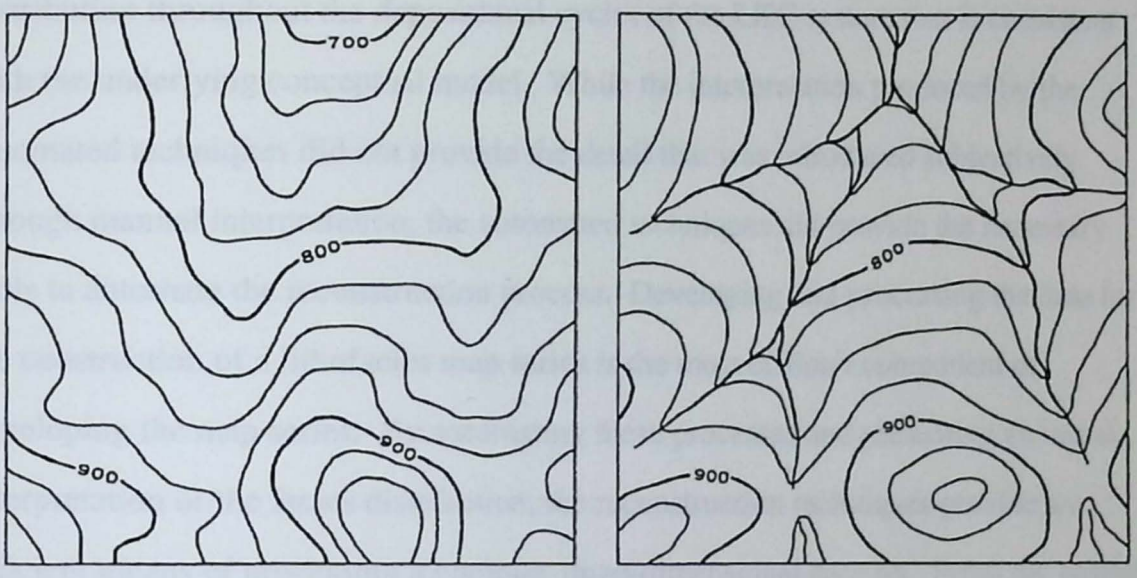

1.) Topographic contour map produced by a computer contouring program.

2.) Topographic contour map produced by manual contouring.

Figure 4.4 - Comparison of computer contouring and manual contouring methods (adapted from Davis, 1986).

Similar to the example presented by Davis (1986), the interpretation presented by the automated reconstruction techniques identifies stratigraphic distribution that lacks the detail introduced through the manually produced interpretation. In order to improve the interpretative capabilities of the automated techniques beyond that demonstrated in this study, the mathematical model would require the incorporation of a complex conceptual rule base. Jones (1986) indicated that better interpretative work can be achieved by integrating automated interpolation tools into the manual interpretative process, rather than through the development of large complex rule bases that are difficult to develop and maintain.

The automated techniques provide the capability to produce a clear, objective, and reproducible interpretation of the facies distribution and the evolution of this

distribution throughout the depositional cycles of the LKC system that is consistent with the underlying conceptual model. While the interpretation produced by the automated techniques did not provide the detail that was introduced subjectively through manual interpretation, the automated techniques did provide the necessary tools to automate the reconstruction process. Developing and processing the data for the construction of a lithofacies map series is the most difficult component of developing the map series. By automating these processes and presenting an initial interpretation of the facies distribution, the reconstruction techniques provide an efficient means of processing a complex three-dimensional data set. From the spatial distribution identified by the automated techniques, a more comprehensive interpretation can be developed manually in a fraction of the time required to develop the same interpretation from raw data. By reducing manual processing of the raw data and providing a more objective initial interpretation, interpretation of lithofacies distribution will be more accurate and reliable.

Chapter Five

CONCLUSIONS AND ADDITIONAL RESEARCH

The reconstruction model developed in this study was intended to provide a more functional capability for automating construction of a two-dimensional lithofacies map series. The reconstruction model uses simple mathematical relationships within the stratigraphic data to identify temporal and three-dimensional relationships within the system. As a result, the reconstruction model does not provide any utility for incorporating phenomena that are not specifically defined within the data, such as regional trend. However, the reconstruction model does provide an effective capability for presenting the stratigraphic distribution over a two-dimensional map series and supporting analysis of the three-dimensional stratigraphic system within the context of the temporal depositional cycle. The map images created by the reconstruction model represent a reasonable interpretation that effectively identifies the stratigraphic distribution from which a more comprehensive manual interpretation can be made in a fraction of the time required without the aid of the reconstruction model. Therefore, the reconstruction model does provide an effective capability for automating construction of the lithofacies map series.

One of the more successful aspects of the approach developed in this study is the simple modular design. The combination data structure that was adopted preserves the well data in simple point data form, while providing the dynamics required for modeling the system at a range of different scales, which may be required under different circumstances where the system may be evaluated from a local or regional scale. This type of structure effectively isolates the data management from

the mathematical processes which ultimately provides a greater degree of adaptability for implementing a broad range of mathematical models. The simple data structure also eliminates the data restructuring that would occur in a more permanent spatial data model resulting from modification in the interpolation operators or in the underlying conceptual model. The combination data model therefore eliminates the complex overhead tied to a more sophisticated structure such as the voxel structure or the three and four dimensional topological structures which makes it easier to develop, implement, and maintain. The flexibility of this approach should also make the reconstruction model relatively simple to adapt to other circumstances where conditions may not be identical to the conditions applied to the reconstruction of the LKC system.

Additional Research

It is difficult to ascertain the evolution of automated reconstruction techniques because this will depend a great deal on the success with which these techniques can be integrated into exploration efforts. Initially, such techniques are intended to automate the reconstruction of lithofacies map series. However, as exploration efforts proceed and these techniques are exercised within an exploration setting, it is likely that automation of the lithofacies map construction will increase understanding of the system which may necessitate the modification of the reconstructive tools. Eventually, it may be advantageous to expand the scientific analysis components of the techniques to include an artificial intelligence capability that could conceivably build a knowledge base by recognizing certain patterns and events that may not be inherently obvious to the scientific observer. This approach could ultimately improve

the reconstructive methods making the automation of these techniques a more viable exploration tool.

The development of an artificial intelligence component to be used in conjunction with the automated techniques would require additional research in two key areas identified in Ris' (1991) definition of "scientific GIS":

1.) Expert System Shell - An expert system shell could be developed that would allow the temporal and interpolation algorithms to use a rule-based system similar to that which an expert or trained geologist would use when reconstructing the system. Temporal and interpolation algorithms which utilize an expert or knowledge based system could provide capabilities to integrate existing knowledge and the dynamic capability to incorporate changes in this knowledge base as they occur.

2.) Event recognition - One of the primary difficulties with integrating the third and fourth dimension lies in the difficulty of recognizing patterns and events within the data. This could be extended to other areas to include recognition of other parameters that may impact the distribution of the stratigraphy or features within the stratigraphy that may influence oil or natural gas production.

Additional research may also be required for some of the principles of the underlying conceptual model. The slice interval reconstructive methods that were adapted from Asquith (1979) assume a uniform depositional rate throughout the system. In reality, shales and carbonates accumulate at different rates which will

effect the temporal evolution identified by the reconstructive process. The conceptual model also assumes that sediment compaction is uniform and constant through the stratigraphic sequence even though there are considerable compactional differences between shales and carbonates. Techniques need to be adapted within the temporal algorithm to incorporate differences in depositional rates and compaction rates to correct the temporal variation that is introduced through these assumptions.

REFERENCES

Al-Taha, Khaled K, and Barrera, Renato, 1990, Temporal data and GIS: An Overview, *GIS/LIS '90 Proceedings*, Vol. 1, pg 244-254.

Aronoff, Stan, 1989, Geographic Information Systems: A Management Perspective, WDL Publications, Ottawa Canada, 294 p.

Asquith, George B., 1979, Subsurface carbonate depositional models: A concise review, PennWell Publishing Company, 121p.

Bader, Christopher D., 1989, Prospective Analysis and Development of the Regressive Depositional Features of the Lansing-Kansas City Groups, Thomas, Gove, and Sheridan Counties, Kansas, 104 p., Unpublished, available upon request.

Beene, Doug, 1993, Personal communication regarding Lansing-Kansas City production, Data provided by the Kansas Geological Survey.

Beller, Aaron, 1991, Spatial/Temporal Events in a GIS, *GIS/LIS '91 Proceedings*, Vol. 2, pg 766-775.

Beller, A., Giblin, T., Le, K.V., Litz, S., Kittel, T., and Schimel, D., 1991, A Temporal GIS prototype for Global Change Research, *GIS/LIS '91 Proceedings*, Vol. 2, pg 752-765.

Burrough, P.A., 1986, Principles of Geographical Information Systems for Land Resources Assessment, *Monographis on Sil and Resources Survey No. 12*, Oxford Science Publications, Oxford University Press, Oxford.

Campbell, J., 1984, Introductory Cartography, Prentice-Hall, Englewood Cliffs, NJ.

Crawford, P.V., and Marks, R.A., 1973, The Visual Effects of Geometric Relationships on Three-Dimensional Maps, *The Professional Geographer*, Vol. 25, No. 3, pp. 233-238.

Dahlberg, E.C., 1972, Aspects of unbiased and biased contouring of geologic data by human and machine operators (obs.), *Geological Society of America*, 1972 Meeting Abstracts with Program, Vol 4, pg 482-483.

Dahlberg, E.C., 1975, Relative effectiveness of geologists and computers in mapping potential hydrocarbon exploration targets, *Mathematical Geology*, Vol 7, pg 373-394.

Davis, Bruce E., Williams, Rhea, 1989, The five dimensions of GIS, *GIS/LIS '89 Proceedings*, Vol. 1, pg 50-58.

Davis, John C., 1973, Statistics and Data Analysis in Geology, Wiley, New York.

Davis, John C., 1986, Statistics and Data Analysis in Geology, Wiley, New York.

DiBiase, David, 1991, Visualization in the Earth Sciences, *Geotimes*, July 1991, pp. 13-15.

Elfick, M.H., 1979, Contouring by use of a triangular mesh, *The Cartographic Journal*, Vol. 16, No. 1, pp. 24-29.

Green, P.J., and Sibson, R., 1978, Computing Dirichlet tesselations in the plane, *The Computer Journal*, Vol. 21, No. 2, pp. 168-173.

Hazelton, N. W.J., Leahy, F.J., and Williamson, I.P., 1990, On the design of temporally-referenced, 3-D Geographical Information Systems: Development of Four-Dimensional GIS, *GIS/LIS '90 Proceedings*, Vol. 1, pg 357-372.

Irwin, J. L., 1965, General theory of epeiric clear water sedimentation, American Association of Petroleum Geologists Bulletin, v. 49, n. 4, p. 445-459.

Jones, Christopher B., 1989, Data structures for three-dimensional spatial information systems in geology, *International Journal of Geographical Information Systems*, Vol. 3, No. 1, pg 15-31.

Jones, T.A., Hamilton, D.E., and Johnson, C.R., 1986, Contouring Geologic Surfaces with the Computer, *Computer Methods in the Geosciences series*, Van Nostrand Reinhold, New York, 314 p.

Junkin, Bobby G., 1982, Development of Three-Dimensional Spatial Displays using a Geographically Based Information System, *Photogrammetric Engineering and Remote Sensing*, Vol. 48, No. 4, April 1982, pp. 577-586.

Langran, Gail, 1989, A review of temporal database research and its use in GIS applications, *International Journal of Geographical Information Systems*, Vol 3, No. 3, pg 215-232.

MacEachren, A.M., and DiBiase D., 1991, Animated Maps of Aggregate Data: Conceptual and Practical Problems, *Cartography and Geographic Information Systems*, Vol. 18, No. 4, pp. 221-229.

McCullagh, Michael J., and Ross, Charles G., 1980, Delauney Triangulation of a Random Data Set for Isarithmic Mapping, *The Cartographic Journal*, Vol. 17, No. 2, pp. 93-99.

Merriam, Daniel F., 1963, The Geologic History of Kansas, *Kansas Geological Survey Bulletin*, No. 162, pp. 178-183

Moellering, Harold, 1980, The Real-Time Animation of Three-Dimensional Maps, *The American Cartographer*, Vol. 7, No. 1, pp. 67-75.

Monmonier, Mark S., 1990, Strategies for the Visualization of Geographic Time-Series Data, *Cartographica*, Vol. 27, No. 1, Spring 1990, pp. 30-45.

Morgan, J.V., 1952, Correlation of radioactive logs of the Lansing and Kansas City Groups in central Kansas, *Journal of Petroleum Technology,* Vol. 4, n. 6, pp. 111-118.

Peuquet, D., 1984, A Conceptual Framework and Comparison of Spatial Data Models, *Cartographica,* Vol. 21, No. 4, pp. 66-113.

Rhynsburger, D., 1973, Analytical Delineation of Thiessen Polygons, *Geographical Analysis,* No. 5, pp. 133-44.

Ris, Fred, 1991, Toward a 'Scientific GIS', *GIS/LIS '91 Proceedings,* Vol. 2, pg 740-751.

Smith, Dennis R., and Paradis, Arthur R., 1989, Three-dimensional GIS for earth sciences, *Three dimensional applications in Geographical Information Systems,* Edited by: Jonathan Raper, Taylor & Francis, pp. 149-154

Todd, R. G., 1976, Oolite-bar progradation, San Andreas Formation, Midland Basin: *American Association of Petroleum Geologists, Bulletin,* Vol. 60, pp. 907-925.

Tufte, E. R., 1983, The Visual Display of Quantitative Information, Graphics Press, Cheshire, Connecticut, pp. 170-175.

Tufte, E. R., 1990, Envisioning Information, Graphic Press, Cheshire, Connecticut, pp. 67-79.

Van Driel, J. Nicholas, 1989, Three dimensional display of geologic data, *Three dimensional applications in Geographical Information Systems,* Edited by: Jonathan Raper, Taylor & Francis, pp. 1-9.

Watney, W.L., 1980, Cyclic sedimentation of the Lansing-Kansas City Groups in northwestern Kansas and southwestern Nebraska, Kansas Geological Survey, Bulletin 220, 72 p.

Watney, W.L., French, J.A., and Franseen, E.K., 1989, Sequence Stratigraphic Interpretations and Modeling of Cyclothems, Kansas Geololgical Society Guidebook, 41st Annual Field Conference, 211 p.

Yoeli, P., 1978, Computer Executed Interpolation of Contours into Arrays of Randomly Distributed Height Points, *The Cartographic Journal,* Vol. 14, No. 2, pp. 103-108.

Youngmann, Carl, 1989, Spatial data structures for modeling subsurface features, *Three dimensional applications in Geographical Information Systems,* Edited by: Jonathan Raper, Taylor & Francis, pp. 129-136.

APPENDIX A - WELL DATA

Naming Conventions and Abbreviations

Regional Formation Descriptions

Abbreviation	Description
K.B.	Kelly Bushing
ANH	Anhydrite
B ANH	Base of Anhydrite
TOP	Topeka
HEEB	Heebner
TOR	Toronto
LKC	Lansing-Kansas City
MARM	Marmaton
PAWN	Pawnee
FT SC	Fort Scott
CHER	Cherokee
MISS	Mississippian
ARB	Arbuckle
RTD	Rotary Total Depth
LTD	Log Total Depth

Lansing-Kansas City Members

Abbreviation	Description
LKC G	Top of G zone regressive carbonate member
LKC G SH	Top of G zone marine shale member
LKC G'	Top of G zone transgressive carbonate member
LKC G' BASE	Base of G zone transgressive carbonate member
LKC H	Top of H zone regressive carbonate member
LKC H SH	Top of H zone marine shale member
LKC H'	Top of H zone transgressive carbonate member
LKC H' BASE	Base of H zone transgressive carbonate member
LKC I	Top of I zone regressive carbonate member
LKC I SH	Top of I zone marine shale member
LKC J	Top of J zone regressive carbonate member
LKC J SH	Top of J zone marine shale member
LKC J'	Top of J zone transgressive carbonate member
LKC J' BASE	Base of J zone transgressive carbonate member
LKC K	Top of K zone regressive carbonate member
LKC K SH	Top of K zone marine shale member
LKC K'	Top of K zone transgressive carbonate member
LKC K' BASE	Base of K zone transgressive carbonate member
LKC L	Top of L zone regressive carbonate member
LKC L SH	Top of L zone marine shale member
LKC L'	Top of L zone transgressive carbonate member
LKC L' BASE	Base of L zone transgressive carbonate member

Lithologic Data

Well Name: #2 DELZEIT
Well Location: 1310 ft from North Line, 1670 ft from West Line, Section 24 T. 010 S., R. 031 W.
X Coord: 4248
Y Coord: 9393
K.B. (ft): 2900

Formation	Depth (ft)	Elevation (ft)
HEEB	3920	-1020
TOR	3942	-1042
LKC	3960	-1060
LKC G	4060	-1160
LKC G SH	4090	-1190
LKC G'	4095	-1195
LKC H	4109	-1209
LKC H SH	4124	-1224
LKC H'	4127	-1227
LKC H' BASE	4131	-1231
LKC I	4137	-1237
LKC I SH	4148	-1248
LKC J	4159	-1259
LKC J SH	4170	-1270
LKC J'	4179	-1279
LKC J' BASE	4180	-1280
LKC K	4187	-1287
LKC K SH	4204	-1304
LKC K'	4212	-1312
LKC L	4217	-1317
LKC L SH	4231	-1331
LKC L'	4239	-1339
MARM	4275	-1375
PAWN	4363	-1463
FT SC	4432	-1532
MISS	4542	-1642
RTD	4570	-1670
LTD	4573	-1673

Well Name: #1 DELZEIT
Well Location: 650 ft from North Line, 1100 ft from West Line, Section 24 T. 010 S., R. 031 W.
X Coord: 4241
Y Coord: 9401
K.B. (ft): 2892

Formation	Depth (ft)	Elevation (ft)
ANH	2459	433
B ANH	2488	404
HEEB	3910	-1018
TOR	3933	-1041
LKC	3948	-1056
LKC G	4050	-1158
LKC G SH	4079	-1187
LKC G'	4084	-1192
LKC H	4098	-1206
LKC H SH	4112	-1220
LKC H'	4115	-1223
LKC H' BASE	4118	-1226
LKC I	4127	-1235
LKC I SH	4138	-1246
LKC J	4149	-1257
LKC J SH	4161	-1269
LKC J'	4169	-1277
LKC J' BASE	4170	-1278
LKC K	4176	-1284
LKC K SH	4194	-1302
LKC K'	4200	-1308
LKC L	4208	-1316
LKC L SH	4220	-1328
LKC L'	4228	-1336
PAWN	4349	-1457
LTD	4397	-1505
RTD	4398	-1506

Well Name: #1 ROBBEN
Well Location: SW/4, SE/4, SE/4, Section 24 T. 010 S., R. 031 W.
X Coord: 4256
Y Coord: 9348
K.B. (ft): 2901

Formation	Depth (ft)	Elevation (ft)
ANH	2467	434
B ANH	2495	406
TOP	3699	-798
HEEB	3924	-1023
TOR	3945	-1044
LKC	3962	-1061
LKC G	4059	-1158
LKC G SH	4091	-1190
LKC G'	4096	-1195
LKC H	4106	-1205
LKC H SH	4120	-1219
LKC H'	4124	-1223
LKC H' BASE	4128	-1227
LKC I	4135	-1234
LKC I SH	4147	-1246
LKC J	4157	-1256
LKC J SH	4171	-1270
LKC J'	4178	-1277
LKC J' BASE	4180	-1279
LKC K	4188	-1287
LKC K SH	4204	-1303
LKC K'	4212	-1311
LKC L	4220	-1319
LKC L SH	4231	-1330
LKC L'	4238	-1337
MARM	4260	-1359
PAWN	4362	-1461
FT SC	4430	-1529
CHER	4459	-1558
MISS	4552	-1651
RTD	4595	-1694
LTD	4596	-1695

Well Name: #1 ENEX-FLIPSE
Well Location: SE/4, SW/4, SW/4, Section 24 T. 010 S., R. 031 W.
X Coord: 4264
Y Coord: 9348
K.B. (ft): 2916

Formation	Depth (ft)	Elevation (ft)
ANH	2484	432
TOP	3712	-796
HEEB	3934	-1018
TOR	3958	-1042
LKC	3976	-1060
LKC E	4041	-1125
LKC G	4070	-1154
LKC G SH	4101	-1185
LKC G'	4106	-1190
LKC H	4116	-1200
LKC H SH	4130	-1214
LKC H'	4135	-1219
LKC H' BASE	4138	-1222
LKC I	4144	-1228
LKC I SH	4156	-1240
LKC J	4167	-1251
LKC J SH	4179	-1263
LKC J'	4187	-1271
LKC J' BASE	4189	-1273
LKC K	4197	-1281
LKC K SH	4215	-1299
LKC K'	4221	-1305
LKC L	4230	-1314
LKC L SH	4240	-1324
LKC L'	4249	-1333
PAWN	4373	-1457
FT SC	4408	-1492
CHER	4432	-1516
MISS	4556	-1640
RTD	4600	-1684

Well Name: #2 ENEX-FLIPSE
Well Location: SE/4, SW/4, SE/4, Section 24 T. 010 S., R. 031 W.
X Coord: 4272
Y Coord: 9348
K.B. (ft): 2919

Formation	Depth (ft)	Elevation (ft)
ANH	2482	437
TOP	3714	-795
HEEB	3934	-1015
TOR	3966	-1047
LKC	3980	-1061
LKC G	4080	-1161
LKC G SH	4109	-1190
LKC G'	4115	-1196
LKC H	4125	-1206
LKC H SH	4138	-1219
LKC H'	4143	-1224
LKC H' BASE	4146	-1227
LKC I	4155	-1236
LKC I SH	4166	-1247
LKC J	4176	-1257
LKC J SH	4187	-1268
LKC J'	4195	-1276
LKC J' BASE	4198	-1279
LKC K	4207	-1288
LKC K SH	4222	-1303
LKC K'	4228	-1309
LKC L	4236	-1317
LKC L SH	4246	-1327
LKC L'	4255	-1336
MARM	4289	-1370
PAWN	4372	-1453
FT SC	4410	-1491
CHER	4432	-1513
MISS	4556	-1637
LTD	4574	-1655
RTD	4575	-1656

Well Name: #3 ENEX-FLIPSE
Well Location: 990 ft from South Line, 2060 ft from East Line, Section 24 T. 010 S., R. 031 W.
X Coord: 4268
Y Coord: 9356
K.B. (ft): 2883

Formation	Depth (ft)	Elevation (ft)
ANH	2458	425
TOP	2694	189
LKC	3960	-1077
LKC G	4057	-1174
LKC G SH	4088	-1205
LKC G'	4094	-1211
LKC H	4104	-1221
LKC H SH	4117	-1234
LKC H'	4122	-1239
LKC H' BASE	4125	-1242
LKC I	4132	-1249
LKC I SH	4143	-1260
LKC J	4156	-1273
LKC J SH	4168	-1285
LKC J'	4177	-1294
LKC J' BASE	4179	-1296
LKC K	4184	-1301
LKC K SH	4200	-1317
LKC K'	4207	-1324
LKC L	4215	-1332
LKC L SH	4224	-1341
LKC L'	4233	-1350
MARM	4274	-1391
PAWN	4364	-1481
FT SC	4398	-1515
CHER	4422	-1539
MISS	4542	-1659
RTD	4596	-1713

Well Name: #23-25 DOUGLAS BIXENMAN
Well Location: NW/4, SW/4, NE/4, Section 25 T. 010 S., R. 031 W.
X Coord: 4240
Y Coord: 9324
K.B. (ft): 2932

Formation	Depth (ft)	Elevation (ft)
TOP	3727	-795
LKC	3986	-1054
LKC G	4082	-1150
LKC G SH	4112	-1180
LKC G'	4116	-1184
LKC H	4130	-1198
LKC H SH	4145	-1213
LKC H'	4148	-1216
LKC H' BASE	4152	-1220
LKC I	4160	-1228
LKC I SH	4171	-1239
LKC J	4180	-1248
LKC J SH	4195	-1263
LKC J'	4205	-1273
LKC J' BASE	4208	-1276
LKC K	4210	-1278
LKC K SH	4230	-1298
LKC K'	4236	-1304
LKC L	4242	-1310
LKC L SH	4253	-1321
LKC L'	4262	-1330
MARM	4304	-1372
PAWN	4384	-1452
FT SC	4422	-1490
CHER	4444	-1512
MISS	4590	-1658
LTD	4907	-1975

Well Name: #24-25 DOUGLAS BIXENMAN
Well Location: NW/4, SW/4, SE/4, Section 25 T. 010 S., R. 031 W.
X Coord: 4240
Y Coord: 9316
K.B. (ft): 2948

Formation	Depth (ft)	Elevation (ft)
LKC	4000	-1052
LKC G	4095	-1147
LKC G SH	4126	-1178
LKC G'	4132	-1184
LKC H	4146	-1198
LKC H SH	4159	-1211
LKC H'	4164	-1216
LKC H' BASE	4166	-1218
LKC I	4174	-1226
LKC I SH	4185	-1237
LKC J	4196	-1248
LKC J SH	4210	-1262
LKC J'	4220	-1272
LKC J' BASE	4223	-1275
LKC K	4226	-1278
LKC K SH	4243	-1295
LKC K'	4250	-1302
LKC L	4257	-1309
LKC L SH	4265	-1317
LKC L'	4276	-1328
MARM	4312	-1364
PAWN	4399	-1451
RTD	4640	-1692

Well Name: #32-25 DOUGLAS BIXENMAN
Well Location: NW/4, NE/4, SW/4, Section 25 T. 010 S., R. 031 W.
X Coord: 4248
Y Coord: 9332
K.B. (ft): 2925

Formation	Depth (ft)	Elevation (ft)
LKC G	4074	-1149
LKC G SH	4106	-1181
LKC G'	4111	-1186
LKC H	4125	-1200
LKC H SH	4139	-1214
LKC H'	4143	-1218
LKC H' BASE	4146	-1221
LKC I	4154	-1229
LKC I SH	4165	-1240
LKC J	4169	-1244
LKC J SH	4188	-1263
LKC J'	4196	-1271
LKC J' BASE	4198	-1273
LKC K	4201	-1276
LKC K SH	4223	-1298
LKC K'	4229	-1304
LKC L	4236	-1311
LKC L SH	4247	-1322
LKC L'	4256	-1331
RTD	4630	-1705

Well Name: #33-25 DOUGLAS BIXENMAN
Well Location: NW/4, SE/4, NW/4, Section 25 T. 010 S., R. 031 W.
X Coord: 4248
Y Coord: 9324
K.B. (ft): 2935

Formation	Depth (ft)	Elevation (ft)
TOP	3721	-786
HEEB	3943	-1008
LKC	3980	-1045
LKC G	4072	-1137
LKC G SH	4107	-1172
LKC G'	4112	-1177
LKC H	4126	-1191
LKC H SH	4140	-1205
LKC H'	4143	-1208
LKC H' BASE	4147	-1212
LKC I	4153	-1218
LKC I SH	4165	-1230
LKC J	4172	-1237
LKC J SH	4188	-1253
LKC J'	4196	-1261
LKC J' BASE	4201	-1266
LKC K	4210	-1275
LKC K SH	4226	-1291
LKC K'	4233	-1298
LKC L	4240	-1305
LKC L SH	4250	-1315
LKC L'	4258	-1323
MARM	4294	-1359
PAWN	4372	-1437
FT SC	4410	-1475
CHER	4434	-1499
MISS	4568	-1633
RTD	4700	-1765

Well Name:	#42-25 DOUGLAS BIXENMAN	
Well Location:	NW/4, NE/4, SE/4, Section 25	T. 010 S., R. 031 W.
X Coord:	4256	
Y Coord:	9332	
K.B. (ft):	2919	

Formation	Depth (ft)	Elevation (ft)
TOP	3716	-797
LKC	3979	-1060
LKC G	4074	-1155
LKC G SH	4105	-1186
LKC G'	4111	-1192
LKC H	4122	-1203
LKC H SH	4136	-1217
LKC H'	4140	-1221
LKC H' BASE	4144	-1225
LKC I	4150	-1231
LKC I SH	4162	-1243
LKC J	4170	-1251
LKC J SH	4185	-1266
LKC J'	4194	-1275
LKC J' BASE	4200	-1281
LKC K	4204	-1285
LKC K SH	4220	-1301
LKC K'	4227	-1308
LKC L	4233	-1314
LKC L SH	4244	-1325
LKC L'	4251	-1332
PAWN	4370	-1451
LTD	4835	-1916

Well Name: #43-25 DOUGLAS BIXENMAN
Well Location: NW/4, SE/4, NE/4, Section 25 T. 010 S., R. 031 W.
X Coord: 4256
Y Coord: 9324
K.B. (ft): 2935

Formation	Depth (ft)	Elevation (ft)
LKC	3983	-1048
LKC A	3983	-1048
LKC A SH	4003	-1068
LKC B	4005	-1070
LKC C	4013	-1078
LKC C SH	4024	-1089
LKC D	4028	-1093
LKC D SH	4048	-1113
LKC E	4056	-1121
LKC G	4081	-1146
LKC G SH	4111	-1176
LKC G'	4116	-1181
LKC H	4129	-1194
LKC H SH	4142	-1207
LKC H'	4146	-1211
LKC H' BASE	4150	-1215
LKC I	4156	-1221
LKC I SH	4169	-1234
LKC J	4181	-1246
LKC J SH	4194	-1259
LKC J'	4202	-1267
LKC J' BASE	4203	-1268
LKC K	4211	-1276
LKC K SH	4229	-1294
LKC K'	4235	-1300
LKC L	4241	-1306
LKC L SH	4252	-1317
LKC L'	4260	-1325
MARM	4293	-1358
PAWN	4374	-1439
CHER	4433	-1498
MISS	4563	-1628
LTD	4620	-1685

Well Name: #52-25 BILL BIXENMAN
Well Location: NE/4, NW/4, SW/4, Section 25 T. 010 S., R. 031 W.
X Coord: 4264
Y Coord: 9332
K.B. (ft): 2938

Formation	Depth (ft)	Elevation (ft)
TOP	3730	-792
LKC	3992	-1054
LKC G	4087	-1149
LKC G SH	4118	-1180
LKC G'	4121	-1183
LKC H	4134	-1196
LKC H SH	4147	-1209
LKC H'	4151	-1213
LKC H' BASE	4155	-1217
LKC I	4161	-1223
LKC I SH	4175	-1237
LKC J	4191	-1253
LKC J SH	4200	-1262
LKC J'	4208	-1270
LKC J' BASE	4210	-1272
LKC K	4212	-1274
LKC K SH	4233	-1295
LKC K'	4239	-1301
LKC L	4246	-1308
LKC L SH	4256	-1318
LKC L'	4263	-1325
MISS	4556	-1618
ARB	4878	-1940
LTD	5369	-2431

Well Name:	#54-25 WILLIAM BIXENMAN	
Well Location:	NE/4, SW/4, SW/4, Section 25	T. 010 S., R. 031 W.
X Coord:	4264	
Y Coord:	9316	
K.B. (ft):	2927	

Formation	Depth (ft)	Elevation (ft)
TOP	3714	-787
LKC	3978	-1051
LKC G	4076	-1149
LKC G SH	4107	-1180
LKC G'	4112	-1185
LKC H	4124	-1197
LKC H SH	4138	-1211
LKC H'	4142	-1215
LKC H' BASE	4146	-1219
LKC I	4152	-1225
LKC I SH	4165	-1238
LKC J	4173	-1246
LKC J SH	4188	-1261
LKC J'	4200	-1273
LKC J' BASE	4202	-1275
LKC K	4206	-1279
LKC K SH	4224	-1297
LKC K'	4230	-1303
LKC L	4236	-1309
LKC L SH	4248	-1321
LKC L'	4256	-1329
PAWN	4375	-1448
RTD	4612	-1685

Well Name: #61-25 WILLIAM BIXENMAN
Well Location: 330 ft from North Line, 1680 ft from East Line, Section 25 T. 010 S., R. 031 W.
X Coord: 4272
Y Coord: 9340
K.B. (ft): 2929

Formation	Depth (ft)	Elevation (ft)
TOP	3724	-795
LKC	3988	-1059
LKC G	4086	-1157
LKC G SH	4115	-1186
LKC G'	4120	-1191
LKC H	4130	-1201
LKC H SH	4146	-1217
LKC H'	4149	-1220
LKC H' BASE	4153	-1224
LKC I	4160	-1231
LKC I SH	4171	-1242
LKC J	4177	-1248
LKC J SH	4193	-1264
LKC J'	4201	-1272
LKC J' BASE	4203	-1274
LKC K	4207	-1278
LKC K SH	4229	-1300
LKC K'	4233	-1304
LKC L	4235	-1306
LKC L SH	4244	-1315
LKC L'	4252	-1323
FT SC	4413	-1484
CHER	4437	-1508
MISS	4552	-1623
RTD	4610	-1681

Well Name:	#63-25 WILLIAM BIXENMAN	
Well Location:	1680 ft from North Line, 1680 ft from East Line, Section 25	T. 010 S., R. 031 W.
X Coord:	4272	
Y Coord:	9324	
K.B. (ft):	2929	

Formation	Depth (ft)	Elevation (ft)
ANH	2490	439
TOP	3721	-792
LKC	3987	-1058
LKC G	4082	-1153
LKC G SH	4113	-1184
LKC G'	4118	-1189
LKC H	4128	-1199
LKC H SH	4142	-1213
LKC H'	4147	-1218
LKC H' BASE	4150	-1221
LKC I	4158	-1229
LKC I SH	4168	-1239
LKC J	4172	-1243
LKC J SH	4191	-1262
LKC J'	4202	-1273
LKC J' BASE	4205	-1276
LKC K	4208	-1279
LKC K SH	4224	-1295
LKC K'	4231	-1302
LKC L	4238	-1309
LKC L SH	4248	-1319
LKC L'	4257	-1328
PAWN	4357	-1428
MISS	4564	-1635
RTD	4612	-1683

Well Name:	#72-25 BILL BIXENMAN	
Well Location:	NE/4, NE/4, SW/4, Section 25	T. 010 S., R. 031 W.
X Coord:	4280	
Y Coord:	9332	
K.B. (ft):	2900	

Formation	Depth (ft)	Elevation (ft)
LKC	3955	-1055
LKC G	4055	-1155
LKC G SH	4087	-1187
LKC G'	4093	-1193
LKC H	4102	-1202
LKC H SH	4116	-1216
LKC H'	4121	-1221
LKC H' BASE	4124	-1224
LKC I	4134	-1234
LKC I SH	4145	-1245
LKC J	4150	-1250
LKC J SH	4166	-1266
LKC J'	4174	-1274
LKC J' BASE	4176	-1276
LKC K	4182	-1282
LKC K SH	4199	-1299
LKC K'	4205	-1305
LKC L	4212	-1312
LKC L SH	4223	-1323
LKC L'	4234	-1334
PAWN	4346	-1446
MISS	4526	-1626
RTD	4568	-1668
LTD	4610	-1710

Well Name:	#68-25 SUMMERS	
Well Location:	SE/4, SW/4, SE/4, Section 25	T. 010 S., R. 031 W.
X Coord:	4272	
Y Coord:	9284	
K.B. (ft):	2928	

Formation	Depth (ft)	Elevation (ft)
TOP	3708	-780
LKC	3910	-982
LKC G	4070	-1142
LKC G SH	4099	-1171
LKC G'	4104	-1176
LKC H	4116	-1188
LKC H SH	4131	-1203
LKC H'	4135	-1207
LKC H' BASE	4138	-1210
LKC I	4147	-1219
LKC I SH	4155	-1227
LKC J	4160	-1232
LKC J SH	4182	-1254
LKC J'	4193	-1265
LKC J' BASE	4196	-1268
LKC K	4199	-1271
LKC K SH	4216	-1288
LKC K'	4222	-1294
LKC L	4230	-1302
LKC L SH	4239	-1311
LKC L'	4246	-1318
PAWN	4367	-1439
MISS	4568	-1640
RTD	4610	-1682

APPENDIX B - PROGRAM SOURCE CODE

Stratigraphic Correlation Program

```
*          This program was designed to stratigraphically correlate the well data
*          to create data arrays for individual time-step files within the TMS.
*          Inidividual horizons are defined within the interface layout.
*
*          The program was designed as a partial fulfillment for a Masters
*          Thesis.
*                              Designed By:     Christopher D. Bader
*                                               Masters Thesis
*                                               Department of Geography
*                                               University of Kansas
*                                               Lawrence, KS  66045
*                                               January 25, 1993
*
*                              Advisor:         Dr. Ling Bian
*
*****************************************************************************
*          Program Input:
*               The program uses data records entered in the DBMS as standard
*               input the records included depende upon a user selectable
*               subset of the entire database.
*****************************************************************************
*          Program Output:
*               Output files are created as individual files
*               for each of the time-steps.  The format for these files
*               is xcoord, ycoord, formation ranking.  Ranking factors are
*               assigned as follows:
*               Regressive Shale           4
*               Regressive Carbonate       3
*               Marine Shale               2
*               Transgressive Carbonate    1
*
*               A separate file is created which identifies the algal mound
*               and shoal facies development.  This file contains development
*               for all wells and all horizons.
*
*****************************************************************************

*****************************************************************
*
*              Initializing Variables and Arrays
*
DEFAULT FILE([Well Header])
ARRAY STRING(20;TimeFm1;0)
ARRAY STRING(20;TimeFm2;0)
ARRAY STRING(20;TimeFm3;0)
ARRAY STRING(20;TimeFm4;0)
ARRAY STRING(20;FmType1;4)
ARRAY STRING(20;FmType2;4)
ARRAY STRING(20;FmType3;4)
ARRAY INTEGER(Fmtyp;3)
LIST TO ARRAY("Formation";TimeFm1)
LIST TO ARRAY("Formation";TimeFm2)
LIST TO ARRAY("Formation";TimeFm3)
LIST TO ARRAY("Formation";TimeFm4)
FmType1{4}:="Regressive Shale"
FmType1{3}:="Regressive Carbonate"
FmType1{2}:="Marine Shale"
```

```
FmType1{1}:="Transgressive Carb"
COPY ARRAY(FmType1;FmType2)
COPY ARRAY(FmType1;FmType3)
DIALOG([Well Header];"TimeSlice Dlog")
If (OK=1)
*****************************************************************
*
*      Correlating Well Data
*
  Fmtyp{1}:=FmType1
  Fmtyp{2}:=FmType2
  Fmtyp{3}:=FmType3
  $vNum:=Records in selection([Well Header])
  ARRAY INTEGER(SliceX;$vNum)
  ARRAY INTEGER(SliceY;$vNum)
  ARRAY INTEGER(Slice;$vNum;100)
  ARRAY STRING(20;WellName;$vNum)
  FIRST RECORD([Well Header])
*
*     Variable $SeqMax is used to determine the extent of the Array Slice
*     to be used for the reconstruction
*
  $SeqMax:=0
  For ($i;1;$vNum)
    $Test:=True
    WellName{$i}:=[Well Header]Well Name
    SliceX{$i}:=[Well Header]X Coord
    SliceY{$i}:=[Well Header]Y Coord
    ARRAY INTEGER(Form;3)
    SEARCH SUBRECORDS([Well Header]Formation Elev;[Well Header]Formation
                      Elev'Formation=TimeFm1{TimeFm1})
    If (Records in subselection([Well Header]Formation Elev)=1)
      Form{1}:=[Well Header]Formation Elev'Depth
    Else
      $Test:=False
    End if
    SEARCH SUBRECORDS([Well Header]Formation Elev;[Well Header]Formation
                      Elev'Formation=TimeFm2{TimeFm2})
    If (Records in subselection([Well Header]Formation Elev)=1)
      Form{2}:=[Well Header]Formation Elev'Depth
    Else
      $Test:=False
    End if
    SEARCH SUBRECORDS([Well Header]Formation Elev;[Well Header]Formation
                      Elev'Formation=TimeFm3{TimeFm3})
    If (Records in subselection([Well Header]Formation Elev)=1)
      Form{3}:=[Well Header]Formation Elev'Depth
    Else
      $Test:=False
    End if
    $FmMax:=Form{3}
    If (TimeFm4#0)
      SEARCH SUBRECORDS([Well Header]Formation Elev;[Well Header]Formation
                        Elev'Formation=TimeFm4{TimeFm4})
      If (Records in subselection([Well Header]Formation Elev)=1)
        INSERT ELEMENT(Form;4;1)
        Form{4}:=[Well Header]Formation Elev'Depth
        $FmMax:=Form{4}
      End if
    End if
*****************************************************************
```

```
*
*              Building the Time-Step Arrays
*
    If ($test)
      For ($r;1;(Size of array(Form)-1))
        For ($j;(Form{1}-Form{$r}+1);(Form{1}-Form{$r+1}+1))
          Slice{$i}{$j}:=Fmtyp{$r}
        End for
      End for
      If ((Form{1}-$FmMax)>$SeqMax)
        $SeqMax:=Form{1}-$FmMax
      End if
      If (Size of array(Form)=4)
        SEARCH SUBRECORDS([Well Header]Formation Elev;[Well Header]Formation
                          Elev'Formation=TimeFm4{TimeFm4})
      Else
        SEARCH SUBRECORDS([Well Header]Formation Elev;[Well Header]Formation
                          Elev'Formation=TimeFm3{TimeFm3})
      End if
      ALL SUBRECORDS([Well Header]Formation Elev'Log Data)
      FIRST SUBRECORD([Well Header]Formation Elev'Log Data)
    End if
    NEXT RECORD([Well Header])
  End for
*****************************************************************
*
*              Writing Output Data for the Regional Facies
*
  For ($j;1;($SeqMax+4);tIncr)
    doc:=Create document("Slice"+String($j-1;0#))
    $PosDev:=0
    For ($i;1;$vNum)
      SEND PACKET(doc;Change string("          ";String(SliceX{$i});(11-
                  Length(String(SliceX{$i})))))
      SEND PACKET(doc;Change string("          ";String(SliceY{$i});(11-
                  Length(String(SliceY{$i})))))
      Case of
        : (Slice{$i}{$j}=0)
          If ($j#1)
            If (Slice{$i}{$j-1}=4)
              Slice{$i}{$j}:=4
            End if
          End if
          SEND PACKET(doc;Change string("     ";String(Slice{$i}{$j});5)+Char(13))
        : (Slice{$i}{$j}<5)
          SEND PACKET(doc;Change string("     ";String(Slice{$i}{$j});5)+Char(13))
        : (Slice{$i}{$j}=5)
          $PosDev:=$PosDev+1
          SEND PACKET(Doc;"    3"+Char(13))
      End case
    End for
    CLOSE DOCUMENT(doc)
  End for
  ARRAY INTEGER(SliceX;0)
  ARRAY INTEGER(SliceY;0)
  ARRAY INTEGER(Slice;0;0)
  ARRAY STRING(20;WellName;0)
End if
```

Vertical Interpolation Program

```
*          This program was designed to re-rank the time-step data to
*          include the vertical dimension for purposes of mapping the
*          paleo-temporal evolution of the facies distribution through
*          the depositional cycles of the Lansing-Kansas City Groups
*
*          The program was designed as a partial fulfillment for a Masters
*          Thesis.
*                         Designed By:    Christopher D. Bader
*                                         Masters Thesis
*                                         Department of Geography
*                                         University of Kansas
*                                         Lawrence, KS  66045
*                                         January 25, 1993
*
*                         Advisor:        Dr. Ling Bian
*
*************************************************************************
*
*          The program uses the following Conventions:
*
*               i,j,k       : represent the x,y, and z components respectively
*               i           : increases from left to right
*               j           : increases from bottom to top
*               k           : increases upward
*
*************************************************************************
*          Program Input:
*               The input files consist of individual files
*               for each of the time-steps.  The format for these files
*               is xcoord, ycoord, formation ranking.  The x and y
*               coordinates identify the Well Location in the user-defined
*               Coordinates.  The Input Rank values are Integer.
*************************************************************************
*          Program Output:
*               The Output files are created as individual files
*               for each of the time-steps.  The format for these files
*               is xcoord, ycoord, formation ranking.  The x and y
*               coordinates identify the Well Location in the user-defined
*               Coordinates provided from the Input file.  The Output Rank
*               Values are Real.
*
*************************************************************************

     PROGRAM VertInt
          Character*32     InFile, Outfile
          Character*15     Root, SliceNm
          Character*17     FileName, FilName2
          Character*2      IndStr
          Character*3      FormStr
          Integer          xCoord(0:50,50),yCoord(0:50,50),Rank(0:50,50)
          Real             Rank2(0:50,50)
          Integer          Interval,MaxInt
          Integer          NPoints,p,k,m,i
          Real             Scale

          Write(5,*) 'Enter Time Slice Interval'
          Read(6,'(I5)') Interval
          Write(5,*) 'Enter the Maximum Time-Slice'
```

```
      Read(6,'(I5)') MaxInt
      Write(5,*) 'Enter the Time-slice file root name (Max of 15 Chars) '
      Read(6,*) Root
      Write(5,*) 'Enter the Number of Wells'
      Read(6,*) NPoints

********
***   Read Input Files
********
      DO 25, k = 0,MaxInt,Interval
            Write(IndStr,'(I2.2)') k
            FileName = TRIM(Root)//IndStr
            Open (39,file=FileName)

            DO 23, p = 1,NPoints
                  Read (39,'(I10,I10,I5)',end = 24)
     &                        xCoord(k,p),yCoord(k,p),Rank(k,p)
23          Continue
24          Close(39)

25    CONTINUE

********
***   Compute the vertical ranking factors
********

      DO 35, p=1,NPoints
            m=0
            write(*,*) 'Well Number ',p
            DO 45, k = 1,MaxInt,Interval
                  IF ((Rank(k,p) <> Rank(k-1,p)) .OR. (k=MaxInt)) THEN
                        Scale = 1.0/DFLOAT(k-1-m)-0.001
                        write(*,*) (k-1-m),Scale
                        n = 0
                        Rank2(m,p) = DFLOAT(Rank(m,p))
                        DO 55, i = m+1,k-1
                              n = n+1
                              Rank2(i,p) = DFLOAT(Rank(i,p)) + n*Scale
55                      CONTINUE
                        m = k
                  END IF
45          CONTINUE
35    CONTINUE

********
***   Write Output Files
********

      DO 75, k = 0,MaxInt,Interval
            Write(IndStr,'(I2.2)') k
            FileName = 'R'//TRIM(Root)//IndStr
            Open (39,file=FileName)

            DO 73, p = 1,NPoints
                  Write (39,'(I10,I10,5X,F5.3)')
     &                  xCoord(k,p),yCoord(k,p),Rank2(k,p)
73          Continue
            Close(39)
75    CONTINUE
      END
```

APPENDIX C - SLICE DATA FILES

Ordinally Ranked Slice Data Files

Slice02

4248	9393	2
4241	9401	2
4256	9348	2
4264	9348	2
4272	9348	2
4268	9356	2
4240	9324	2
4240	9316	2
4248	9332	2
4248	9324	2
4256	9332	2
4256	9324	2
4264	9332	2
4264	9316	2
4272	9340	2
4272	9324	2
4280	9332	2
4272	9284	2

Slice04

4248	9393	2
4241	9401	2
4256	9348	2
4264	9348	2
4272	9348	2
4268	9356	2
4240	9324	2
4240	9316	2
4248	9332	2
4248	9324	2
4256	9332	2
4256	9324	2
4264	9332	2
4264	9316	2
4272	9340	2
4272	9324	2
4280	9332	2
4272	9284	2

Slice06

4248	9393	2
4241	9401	2
4256	9348	2
4264	9348	2
4272	9348	2
4268	9356	2
4240	9324	2
4240	9316	2
4248	9332	2
4248	9324	2
4256	9332	2
4256	9324	2
4264	9332	2
4264	9316	2
4272	9340	2
4272	9324	2
4280	9332	2
4272	9284	2

Slice08

4248	9393	3
4241	9401	3
4256	9348	3
4264	9348	2
4272	9348	2
4268	9356	2
4240	9324	2
4240	9316	2
4248	9332	2
4248	9324	3
4256	9332	3
4256	9324	3
4264	9332	3
4264	9316	3
4272	9340	3
4272	9324	2
4280	9332	2
4272	9284	3

Slice10

4248	9393	3
4241	9401	3
4256	9348	3
4264	9348	3
4272	9348	3
4268	9356	3
4240	9324	3
4240	9316	2
4248	9332	3
4248	9324	3
4256	9332	3
4256	9324	3
4264	9332	3
4264	9316	3
4272	9340	3
4272	9324	3
4280	9332	2
4272	9284	3

Slice12

4248	9393	3
4241	9401	3
4256	9348	3
4264	9348	3
4272	9348	3
4268	9356	3
4240	9324	3
4240	9316	3
4248	9332	3
4248	9324	3
4256	9332	3
4256	9324	3
4264	9332	3
4264	9316	3
4272	9340	3
4272	9324	3
4280	9332	3
4272	9284	3

Slice14

4248	9393	3
4241	9401	3
4256	9348	3
4264	9348	3
4272	9348	3
4268	9356	3
4240	9324	3
4240	9316	3
4248	9332	3
4248	9324	3
4256	9332	3
4256	9324	3
4264	9332	3
4264	9316	3
4272	9340	3
4272	9324	3
4280	9332	3
4272	9284	3

Slice16

4248	9393	3
4241	9401	3
4256	9348	3
4264	9348	3
4272	9348	3
4268	9356	3
4240	9324	3
4240	9316	3
4248	9332	3
4248	9324	3
4256	9332	3
4256	9324	3
4264	9332	3
4264	9316	3
4272	9340	3
4272	9324	3
4280	9332	3
4272	9284	4

Slice18

4248	9393	3
4241	9401	3
4256	9348	4
4264	9348	3
4272	9348	4
4268	9356	4
4240	9324	3
4240	9316	3
4248	9332	3
4248	9324	4
4256	9332	4
4256	9324	3
4264	9332	4
4264	9316	3
4272	9340	4
4272	9324	3
4280	9332	3
4272	9284	4

Slice20

4248	9393	3
4241	9401	4
4256	9348	4
4264	9348	4
4272	9348	4
4268	9356	4
4240	9324	3
4240	9316	4
4248	9332	3
4248	9324	4
4256	9332	4
4256	9324	4
4264	9332	4
4264	9316	3
4272	9340	4
4272	9324	4
4280	9332	3
4272	9284	4

Slice22

4248	9393	3
4241	9401	4
4256	9348	4
4264	9348	4
4272	9348	4
4268	9356	4
4240	9324	4
4240	9316	4
4248	9332	4
4248	9324	4
4256	9332	4
4256	9324	4
4264	9332	4
4264	9316	4
4272	9340	4
4272	9324	4
4280	9332	4
4272	9284	4

Vertically Ranked Slice Data Files

Slice02			***Slice04***			***Slice06***		
4248	9393	2.284	4248	9393	2.567	4248	9393	2.851
4241	9401	2.284	4241	9401	2.567	4241	9401	2.851
4256	9348	2.331	4256	9348	2.663	4256	9348	2.994
4264	9348	2.248	4264	9348	2.496	4264	9348	2.744
4272	9348	2.248	4272	9348	2.496	4272	9348	2.744
4268	9356	2.248	4268	9356	2.496	4268	9356	2.744
4240	9324	2.248	4240	9324	2.496	4240	9324	2.744
4240	9316	2.198	4240	9316	2.396	4240	9316	2.594
4248	9332	2.248	4248	9332	2.496	4248	9332	2.744
4248	9324	2.284	4248	9324	2.567	4248	9324	2.851
4256	9332	2.331	4256	9332	2.663	4256	9332	2.994
4256	9324	2.284	4256	9324	2.567	4256	9324	2.851
4264	9332	2.331	4264	9332	2.663	4264	9332	2.994
4264	9316	2.284	4264	9316	2.567	4264	9316	2.851
4272	9340	2.284	4272	9340	2.567	4272	9340	2.851
4272	9324	2.248	4272	9324	2.496	4272	9324	2.744
4280	9332	2.198	4280	9332	2.396	4280	9332	2.594
4272	9284	2.398	4272	9284	2.796	4272	9284	3.000

Slice08			***Slice10***			***Slice12***		
4248	9393	3.000	4248	9393	3.141	4248	9393	3.282
4241	9401	3.000	4241	9401	3.180	4241	9401	3.360
4256	9348	3.099	4256	9348	3.297	4256	9348	3.495
4264	9348	2.992	4264	9348	3.110	4264	9348	3.330
4272	9348	2.992	4272	9348	3.124	4272	9348	3.372
4268	9356	2.992	4268	9356	3.124	4268	9356	3.372
4240	9324	2.992	4240	9324	3.090	4240	9324	3.270
4240	9316	2.792	4240	9316	2.990	4240	9316	3.142
4248	9332	2.992	4248	9332	3.090	4248	9332	3.270
4248	9324	3.000	4248	9324	3.220	4248	9324	3.440
4256	9332	3.110	4256	9332	3.330	4256	9332	3.551
4256	9324	3.000	4256	9324	3.198	4256	9324	3.396
4264	9332	3.110	4264	9332	3.330	4264	9332	3.551
4264	9316	3.000	4264	9316	3.165	4264	9316	3.329
4272	9340	3.000	4272	9340	3.248	4272	9340	3.496
4272	9324	2.992	4272	9324	3.099	4272	9324	3.297
4280	9332	2.792	4280	9332	2.990	4280	9332	3.099
4272	9284	3.220	4272	9284	3.440	4272	9284	3.661

Slice14			***Slice16***			***Slice18***		
4248	9393	3.423	4248	9393	3.563	4248	9393	3.704
4241	9401	3.539	4241	9401	3.719	4241	9401	3.899
4256	9348	3.693	4256	9348	3.891	4256	9348	4.000
4264	9348	3.551	4264	9348	3.771	4264	9348	3.991
4272	9348	3.620	4272	9348	3.868	4272	9348	4.000
4268	9356	3.620	4268	9356	3.868	4268	9356	4.000
4240	9324	3.450	4240	9324	3.629	4240	9324	3.809
4240	9316	3.426	4240	9316	3.709	4240	9316	3.993
4248	9332	3.450	4248	9332	3.629	4248	9332	3.809
4248	9324	3.661	4248	9324	3.881	4248	9324	4.000
4256	9332	3.771	4256	9332	3.991	4256	9332	4.166
4256	9324	3.594	4256	9324	3.792	4256	9324	3.990
4264	9332	3.771	4264	9332	3.991	4264	9332	4.166
4264	9316	3.494	4264	9316	3.659	4264	9316	3.823
4272	9340	3.744	4272	9340	3.992	4272	9340	4.166
4272	9324	3.495	4272	9324	3.693	4272	9324	3.891
4280	9332	3.297	4280	9332	3.495	4280	9332	3.693
4272	9284	3.881	4272	9284	4.000	4272	9284	4.284

Slice20			***Slice22***		
4248	9393	3.845	4248	9393	3.986
4241	9401	4.000	4241	9401	4.665
4256	9348	4.398	4256	9348	4.796
4264	9348	4.249	4264	9348	4.747
4272	9348	4.398	4272	9348	4.796
4268	9356	4.398	4268	9356	4.796
4240	9324	3.989	4240	9324	4.499
4240	9316	4.249	4240	9316	4.747
4248	9332	3.989	4248	9332	4.499
4248	9324	4.398	4248	9324	4.796
4256	9332	4.497	4256	9332	4.828
4256	9324	4.249	4256	9324	4.747
4264	9332	4.497	4264	9332	4.828
4264	9316	3.988	4264	9316	4.499
4272	9340	4.497	4272	9340	4.828
4272	9324	4.000	4272	9324	4.665
4280	9332	3.891	4280	9332	4.000
4272	9284	4.567	4272	9284	4.851